

**New determination of proton spectroscopic factors and reduced widths for  $^8\text{Be}$  states in the 16.5 – 18.0 MeV excitation energy region via the study of the  $^7\text{Li}(^3\text{He},d)^8\text{Be}$  transfer reaction at  $E_{lab} = 20 \text{ MeV}$ .**

A. Belhout,<sup>1</sup> S. Ouichaoui\*,<sup>1</sup> H. Beaumevieille,<sup>1</sup> A. Bouchemha,<sup>1</sup> G. Bogaert,<sup>2</sup> S. Fortier,<sup>3</sup> J. Kiener,<sup>2</sup> A. Lefebvre-Schuhl,<sup>2</sup> J. M. Maison,<sup>3</sup> L. Rosier,<sup>3</sup> J. Rotbard,<sup>3</sup> V. Tatischeff,<sup>2</sup> J.P. Thibaud,<sup>2</sup> and J. Verlotte<sup>3</sup>

<sup>1</sup>*Université des Sciences et de la Technologie Houari Boumediene (USTHB),  
Faculté de Physique, BP 32, El-Alia,  
16111 Bab Ezzouar, Algiers, Algeria,*

<sup>2</sup>*Centre de Sciences Nucléaires et des Sciences de la Matière (CSNSM),  
IN2P3/CNRS-Université de Paris XI, 91405 Campus Orsay France,*

<sup>3</sup>*Institut de Physique Nucléaire, IN2P3/CNRS-Université  
de Paris XI, 91406 Orsay Cedex, France,*

(Dated: July 2017)

## Abstract

The angular distributions of  ${}^8\text{Be}$  states in the excitation energy region,  $E_x \sim (16.5 - 18.2)$  MeV, produced in the  ${}^7\text{Li}({}^3\text{He},d){}^8\text{Be}$  proton transfer reaction have been measured at the Orsay 14.8-MV tandem accelerator for  ${}^3\text{He}^{2+}$  ion bombarding energy,  $E_{lab} = 20$  MeV, and forward angular range,  $\theta_{lab} = 5^\circ - 50^\circ$ . A high energy resolution detection system composed of a split-pole magnetic spectrometer and a  $\Delta E - E$ , position-sensitive drift chamber was used to record the energy spectra of outgoing deuterons. The measured cross section data for the direct reaction component have been separated from the compound nucleus one, then analyzed in the framework of the non local, FR-DWBA theory. New values of the  $C^2S$  and  $(S_{p1/2}, S_{p3/2})$  proton absolute and partial spectroscopic factors and related  $\gamma_p^2(a)$  proton reduced widths versus the  $p + {}^7\text{Li}$  channel radius have been extracted for the  $2^+(16.626)$  and  $2^+(16.922)$ ,  $T = 0 + 1$  isospin-mixed loosely bound states of astrophysical interest and the  $1^+(17.640)$ ,  $T = 1$  unbound state of  ${}^8\text{Be}$ . They are compared to sparse earlier experimental values and to shell-model predicted ones from the literature, and are discussed. In particular, the status of the spectroscopic information on the  $2^+$  isospin-mixed doublet is reviewed and up-dated. The application in nuclear astrophysics of the DWBA derived results is emphasised.

PACS numbers: 25.55.Hp; 24.10.Eq; 27.20.+n; 26.20.Cd; 26.35.+c.

Keywords:  ${}^7\text{Li}({}^3\text{He},d){}^8\text{Be}$  reaction,  $E_{3He}(\text{lab}) = 20$  MeV: DWBA analysis; deduced  $S_p$ , reduced  $\gamma_p^2$ . Big-bang and stellar nucleosyntheses,

## Contents

<b>I. Introduction</b>	1
<b>II. Experimental details, procedures, results and discussions</b>	5
A. Experimental set up and procedure	5
B. Target thickness determination	6
C. Analysis of the deuteron energy spectra	6
D. Experimental angular distributions	9
<b>III. Analysis of cross section data, results and discussion</b>	13
A. FR-DWBA analysis of angular distribution data	13
B. Results and discussion	14
1. Angular distributions	14
2. Proton spectroscopic factors	15
3. $\gamma_p^2(a)$ proton reduced widths	19
<b>IV. Summary and conclusions</b>	22
<b>References</b>	24

## I. INTRODUCTION

The spectroscopic information on nuclear energy levels (excitation energies, spectroscopic factors, particle reduced widths,..) is crucial in nuclear physics regarding the structure of light and heavier nuclei. It is intensively used for describing, modeling and elucidating many nuclear structure problems such as isobaric analogue states, rotational bands, isospin mixing, two-level systems,  $\alpha$ -particle clustering or exotic nuclear states (see [1–5] and references therein). This information is also of great interest to nuclear astrophysics where nuclear levels of particular structure often play a prominent role in big bang and/or in stellar nucleosyntheses (BBN, SN) [6–8]. This is the case, for example, of the  $J^\pi = 2^+$ ,  $T = 1$  ground states of  ${}^8\text{Li}$  and  ${}^8\text{B}$  nuclei and the two  $2^+$ ,  $T = 0 + 1$  isospin-mixed states in the two  $\alpha$ -cluster  ${}^8\text{Be}$  nucleus at  $E_x = 16.626$  MeV and  $16.922$  MeV below the  $p + {}^7\text{Li}$  threshold ( $E_x = 17.255$  MeV) [9–15]. In particular, the latter two loosely bound states are involved

in the resonant  ${}^7\text{Li}(p,\alpha){}^4\text{He}$  hydrogen burning reaction implied both in BBN and in SN, whose cross section at stellar energies is small ( $\sigma = (4.3 \pm 0.9) \times 10^{-5}$  mb at  $E_p = 28.1$  keV) and difficult to measure directly due mainly to the inhibitory effect of the  $p + {}^7\text{Li}$  Coulomb barrier ( $B_c = 2.473$  MeV). Alternatively, the spectroscopic information on the latter two  $2^+$  states, notably their proton reduced widths, should be much more easily accessible via the  ${}^7\text{Li}({}^3\text{He},d){}^8\text{Be}$  transfer reaction. Indeed, the cross section of the latter reaction is large and the properties of  ${}^8\text{Be}$  states can be more easily derived from it provided the energy of the incident  ${}^3\text{He}^{2+}$  ion beam is sufficiently high for the direct interaction mechanism to be dominating over the ( ${}^{10}\text{B}$ ) compound nucleus formation. Then, the astrophysical  $S(E)$  – factor and the stellar rate of the  ${}^7\text{Li}(p,\alpha){}^4\text{He}$  proton capture reaction may be efficiently determined indirectly via the measurement of the  ${}^7\text{Li}({}^3\text{He},d){}^8\text{Be}$  transfer reaction angular distributions. Besides, other indirect methods (such as the asymptotic normalization coefficient (ANC), the trojan-horse (TH) and the Coulomb break-up methods [16]) can be also used to reach the same objectives. Furthermore regarding astrophysical applications, the most precise possible determination of the rates of nuclear reactions involving the  ${}^6,{}^7\text{Li}$  and  ${}^7,{}^8\text{Be}$  isotopes and considered in BBN calculations have been recommended (see, e.g., [17] and references therein). The objective in sight was to study the origin of discrepancies between the observed abundance of  ${}^7\text{Li}$  in metal-poor galactic halo dwarf stars and its predicted primordial abundance ( ${}^7\text{Li}/\text{H} = (1.58 \pm 0.314) \times 10^{-10}$  [18] and  $(4.68 \pm 0.67) \times 10^{-10}$  [19], respectively), and between an assumed to be observed value [20] of the Lithium isotopic ratio and its predicted one ( ${}^6\text{Li}/{}^7\text{Li} \sim 10^{-5}$  [21]). However, an experiment of the LUNA collaboration [22] constraining the  ${}^2\text{H}(\alpha,\gamma){}^6\text{Li}$  reaction cross section yielded a value of this ratio,  ${}^6\text{Li}/{}^7\text{Li} = (1.5 \pm 0.3) \times 10^{-5}$ , matching the BBN prediction [21], which has been also confirmed recently by theoretical calculations [23]. Then, as highlighted by Coc in [24], while a BBN  ${}^6\text{Li}$  problem is no longer up-to-date, only the  ${}^7\text{Li}$  problem still persists presently. But among other hardly searched for solutions (see [24] and references therein), the perspective of solving the latter puzzle via nuclear reaction rate evaluations seems not to hold any more actually [24]. Note, besides, that following the recent observation of a  $6.8\sigma$  anomaly at  $E_x \sim 17$  MeV in  ${}^8\text{Be}$  [25] decaying via internal electron-positron pair creation, further perspectives for a particle physics solution to the cosmological Lithium problem have been proposed (see [26] and references therein).

In one-step transfer reactions such as the  ${}^7\text{Li}({}^3\text{He},d){}^8\text{Be}$  one - e.g., proton stripping in

(d,n) and ( $^3\text{He}$ ,d) reactions or  $\alpha$ -particle stripping in ( $^6\text{Li}$ ,d) and ( $^7\text{Li}$ ,t) reactions - one particle is selectively transferred from the projectile into a given shell of the final nucleus with definite  $n\ell j$  quantum numbers without altering the target nucleus core [27]. Such direct reactions have been used since long as privileged tools in order to precisely determine the level parameters (excitation energies, widths,  $J^\pi$  values) for many involved residual nuclei. The accumulated experimental data on the energy levels of the  $A = 8 - 10$  light nuclei has been reported in the successive compilations by Ajzenberg-Selove and Tilley et al. (see [28] and references therein). Many nuclear reactions and various experimental methods have been used for determining the parameters of the peculiar  $2^+$  isospin-mixed doublet of  $^8\text{Be}$ . However, inconsistencies between the results from different groups have been observed due evenly to the complexity of the investigated nuclear interaction processes involving interference effects. Thus, the spectroscopic information on  $^8\text{Be}$  states in the excitation energy region,  $E_x \sim (16.5 - 18)$  MeV, is yet lacking in the literature and some nuclear reactions involving the  $2^+$  isospin-mixed doublet have not been sufficiently explored. Especially, only few measurements have been carried out previously [10, 29–31] on the  $^7\text{Li}(^3\text{He},\text{d})^8\text{Be}$  transfer reaction with cross section experimental data being reported only in reference [30]. Indeed, Marion et al. [10] have measured a unique deuteron energy spectrum at a laboratory angle,  $\theta_{lab} = 40^\circ$ , for  $^3\text{He}$  ion bombarding energy,  $E_{lab} = 10.972$  MeV, in order to determine the total widths of the  $2^+(16.626)$  and  $2^+(16.922)$  states of  $^8\text{Be}$ . The study of this reaction by Piluso et al. [29] was limited to recording only two deuteron energy spectra at two laboratory angles,  $\theta_{lab} = 10^\circ$  and  $25^\circ$ , for a  $^3\text{He}$  ion bombarding energy,  $E_{lab} = 15$  MeV, which were used to determine level parameters for the above two  $2^+$  states of  $^8\text{Be}$  with pointing out their interference contributions and to search for  $1p-1h$  states. Besides, Basak et al. [30] have measured the  $^7\text{Li}(\overrightarrow{^3\text{He}},\text{d})^8\text{Be}$  reaction angular distributions for polarized  $^3\text{He}$  ions of incident energy,  $E_{lab} = 33.3$  MeV. The analysis of the latter data within the DWBA formalism has led these authors to derive the only available  $C^2S_{global}$  proton spectroscopic factor experimental values for the  $2^+(16.626)$ ,  $1^+(17.64)$  and  $1^+(18.15)$  states of  $^8\text{Be}$  from this reaction, to our knowledge, while the  $2^+(16.922)$  state seemed to be not clearly populated in that experiment. Finally, Cocke has reported [31] a global experimental angular distribution for the  $2^+(16.626)$  state measured at  $E_{lab} = 10$  MeV where the direct and compound nucleus contributions were not separated. Then, despite many efforts devoted to study the  $2^+$ ,  $T = 0 + 1$  isospin-mixed doublet of  $^8\text{Be}$  (see [9–12, 28–31] and references therein), not

only the corresponding spectroscopic information remains incomplete but the structures of these two special states steadily seem to be complex and not well elucidated. On the other hand concerning the reaction mechanism prevailing at thermonuclear temperatures in the  ${}^7\text{Li}(p,\alpha){}^4\text{He}$  proton capture reaction, a previous DWBA analysis [32] of precise cross section experimental data available for  $E_p = (13 - 10^3)$  keV proton energies [32, 33] have led the authors to an apparently good agreement between theory and experiment, thus suggesting to interpret the data in terms of a dominant three-nucleon direct reaction transfer. However, this conclusion contradicts existing clear evidences for  ${}^8\text{Be}$  compound nucleus formation in this reaction, as will be detailed later in Section III. Therefore, the  ${}^7\text{Li}(p,\alpha){}^4\text{He}$  reaction cross section experimental data can be more pertinently analysed, instead, in the framework of the R-Matrix theory with assuming the predominance of ( ${}^8\text{Be}$ ) compound nucleus reaction mechanism. In particular, the  $\gamma_p^2(a)$  proton reduced widths for  ${}^8\text{Be}$  states (mainly the  $2^+$  isospin-mixed doublet) derived as free fit parameters in such analysis deserve to be compared to experimental counterparts from the  ${}^7\text{Li}({}^3\text{He},d){}^4\text{He}$  or  ${}^7\text{Li}(d,n){}^8\text{Be}$  proton stripping reactions and to shell model predictions [34]. It therefore appeared to us worthwhile to critically re-visit the spectroscopy of  ${}^8\text{Be}$  nucleus states within the (16.5 – 18.2) MeV excitation energy region including the  $2^+$ ,  $T = 0 + 1$  isospin mixed doublet. For all these reasons, we have undertaken the measurement of the  ${}^7\text{Li}({}^3\text{He},d){}^8\text{Be}$  reaction angular distributions for  ${}^3\text{He}^{2+}$  ion bombarding energy,  $E_{lab} = 20$  MeV. In this work, we thus preferentially aimed at performing a new and reliable experimental determination of the  $C^2S$  spectroscopic factors for these two  $2^+$  states of astrophysical interest and deriving relevant values of the closely related proton reduced widths,  $\gamma_p^2$ , that can be very useful, e.g., for constraining the number of fit parameters in the R-Matrix analyses of cross section experimental data for fusion reactions involving  ${}^8\text{Be}$  states.

A high energy resolution, position-sensitive detection system was used in the experiment that will be described in Section II. The contents of the direct interaction component within the recorded energy spectra of the outgoing deuterons have been separated from the compound nucleus contribution and transformed into corresponding center of mass cross sections. Then, the latter angular distribution experimental data have been carefully analyzed in the framework of the non-local, finite-range DWBA formalism. A detailed account of the performed theoretical analysis of the  ${}^7\text{Li}({}^3\text{He},d){}^8\text{Be}$  angular distribution experimental data is given in Section III where the derived  $C^2S$  and  $\gamma_p^2$  data for the three excited states

of  $^8\text{Be}$  considered here, i.e., the  $2^+(16.626)$ ,  $2^+(16.922)$  and  $1^+(17.64)$  states, are reported and discussed. Finally, a summary and conclusions are given in Section IV.

## II. EXPERIMENTAL DETAILS, PROCEDURES, RESULTS AND DISCUSSIONS

### A. Experimental set up and procedure

The experimental set up and detection system were the same as in our previous experiment on the  $^{12}\text{C}(^6\text{Li},\text{d})^{16}\text{O}$   $\alpha$ -transfer reaction [35]. Then, mainly specific aspects to the current  $^7\text{Li}(^3\text{He},\text{d})^8\text{Be}$  experiment are emphasized in this section.

The experiment was carried out at the Orsay-Institut de Physique Nucléaire MP Tandem accelerator, on the line of the Enge split-pole magnetic spectrometer [36]. A 20 MeV  $^3\text{He}^{2+}$  ion beam delivered with high energy resolution ( $\Delta E/E \approx 2 \times 10^{-4}$ ) and average beam current intensity of  $\sim 100$  nA was directed onto a self-supporting,  $49 \mu\text{g}\cdot\text{cm}^{-2}$ -thick target foil of natural lithium placed under high vacuum in the reaction chamber at the object focal point of the magnetic spectrometer. The target was prepared by vacuum evaporation of metallic lithium. Before being used in the experiment, it was continuously maintained under vacuum in order to reduce its oxidation and/or contamination by chemical impurities until it was introduced into the reaction chamber by means of a sieve without breaking the vacuum. The nuclear reaction products were, first, momentum analyzed by the magnetic spectrometer whose horizontal entrance aperture was set at  $\pm 1.5^\circ$  corresponding to a solid angle,  $\Delta\Omega$ , of  $\sim 1.6$  msr. Then, they were identified in the spectrometer image focal plane by a detection system of 70 cm length composed of three successive detectors [37]: (i) a position sensitive 128– anode wires drift chamber giving the position,  $X$ , of particle impacts, (ii) a proportional counter measuring the particle energy loss,  $\Delta E$ , and (iii) a plastic scintillator (associated to a photomultiplier tube through a light-guide) measuring the particle residual energy,  $E' = E - \Delta E$ . Both the target thickness and the beam current intensity (the latter was measured by a well shielded and isolated Faraday cup) were continuously monitored during the whole experiment by means of a 100  $\mu\text{m}$ – thick surface barrier Si detector placed inside the reaction chamber at  $\theta_{lab} = 42^\circ$  relative to the incident beam direction. The  $^7\text{Li}(^3\text{He},\text{d})^8\text{Be}$  reaction angular distributions were measured by recording energy spectra of the outgoing deuterons over the forward angular range,  $5^\circ \leq \theta_{lab} \leq 50^\circ$ , in  $5^\circ$  steps.

## B. Target thickness determination

The thickness of the used Li target has been determined as follows. The energy spectra for 25 MeV  ${}^3\text{He}^{++}$  ions elastically scattered off a LiF target were registered at observation angles,  $\theta_{lab} = 36^\circ, 39^\circ, 42^\circ, 45^\circ$  and  $48^\circ$  with the magnetic spectrometer being set to focus onto the detector the  ${}^3\text{He}$  particles scattered off  ${}^{19}\text{F}$  nuclei. The number of these nuclei in the LiF target,  $N({}^{19}\text{F}) = (35.07 \pm 01.46) \times 10^{17} \text{cm}^{-2}$ , was derived from the  ${}^{19}\text{F}({}^3\text{He}, {}^3\text{He}){}^{19}\text{F}$  elastic scattering cross sections measured previously [38] at the same ion energy and laboratory angles. Consideration of the energy spectra from the monitor detector and of the accumulated beam charge showed that the target remained stable during these elastic scattering measurements. Assuming the conservation of the stoichiometric ratio during the fabrication of the LiF target leads to  $N({}^{19}\text{F}) = N(\text{Li})$ . Then, setting the spectrometer such that the  ${}^3\text{He}$  particles scattered off Li nuclei were focused onto the detector, two spectra for elastically scattered 25 MeV  ${}^3\text{He}^{++}$  ions were registered at  $\theta_{lab} = 36^\circ$ : one with the LiF target in place, the other with the metallic Li target. Then, the comparison of the areas of the elastic scattering peaks leads to the number of Li nuclei contained in the metallic Li target,  $N(\text{Li}) = (42.80 \pm 02.00) \times 10^{17} \text{cm}^{-2}$ , i.e., to a thickness of  $\sim 49 \pm 3 \mu\text{g cm}^{-2}$ . One then deduces the number of  ${}^7\text{Li}$  nuclei to be  $N({}^7\text{Li}) = (39.64 \pm 01.84) \times 10^{17} \text{cm}^{-2}$ . Note that the ratio of the number of Li nuclei in the metallic Li target to those in the LiF target,  $N(\text{Li})_{\text{Li target}}/N(\text{Li})_{\text{LiF target}}$ , amounts to  $1.22 \pm 0.08$ , this value being obtained without taking into account the information from the Si monitor detector. It is in very good agreement with the ratio,  $A(\text{Li})_{\text{Li target}}/A(\text{Li})_{\text{LiF target}} = 1.21 \pm 0.02$ , with A denoting the ratio of the number of counts of Li nuclei to the accumulated beam charge, Q (corrected for the dead-time), from the monitor detector, i.e.,  $A = (N'_{\text{counts}}(\text{Li})/Q)_{\text{Monitor}}$ .

## C. Analysis of the deuteron energy spectra

Despite the precautions taken during the fabrication and handling of the Li target, the deuteron energy spectra exhibited significant contamination in  ${}^{12}\text{C}$ ,  ${}^{14}\text{N}$ ,  ${}^{16}\text{O}$  and  ${}^{19}\text{F}$ . Then, peaks corresponding to ( ${}^3\text{He}$ , d) proton stripping reactions on the corresponding nuclei giving, respectively,  ${}^{13}\text{N}$ ,  ${}^{15}\text{O}$ ,  ${}^{17}\text{F}$  and  ${}^{20}\text{Ne}$  as residual nuclei have been observed. Part of the deuteron energy spectrum taken at  $\theta_{lab} = 5^\circ$  and showing deuteron peaks corresponding



to the states of  ${}^8\text{Be}$  at  $E_x = 16.626$  MeV ( $2^+$ ), 16.922 MeV ( $2^+$ ), 17.640 MeV ( $1^+$ ) and 18.150 MeV ( $1^+$ ) is reported in Fig. 1. Note, however, that owing to the fact that the peak associated with the relatively broad ( $\Gamma_{cm} = 138 \pm 6$  keV [28])  $1^+(18.150)$ ,  $T = 1$  state was more critically affected by contaminant peaks from secondary reactions, this state was not considered in the current study. In all the measured deuteron energy spectra, the peaks associated with the two  $2^+$  (16.626) and  $2^+(16.922)$  states of main concern here were quite well separated due to the high energy resolution of the detection system used, with the peak for the former state being considerably more intense than the one for the latter state (see also Fig. 2). Furthermore, consistently with kinematics predictions, these two peaks did not suffer severe contamination, notably from the  ${}^{16}\text{O}({}^3\text{He},d){}^{17}\text{F}$  reaction beyond  $\theta_{lab} \sim 15^\circ$ . While the contents of the peaks associated with the narrow  $1^+(17.640)$ , ( $T = 1$ ) state ( $\Gamma_{cm} = 10.7 \pm 0.5$  keV [10, 28]) were extracted easily, those of the peaks for the  $2^+(16.626)$  and  $2^+(16.922)$  states required a special treatment. Indeed, as indicated, these two final states are both characterized by an important  $T = 0 + 1$  isospin mixing [9–11]. Then, their respective wave functions can be written as (see [10])

$$|16.626 \text{ MeV}\rangle = A |T = 0\rangle + B |T = 1\rangle \quad (1)$$

$$|16.922 \text{ MeV}\rangle = B |T = 0\rangle - A |T = 1\rangle \quad (2)$$

where the coefficients ( $A$ ,  $B$ ) represent respective weights of the  $|T = 0\rangle$  and  $|T = 1\rangle$  isospin contributions, expected to have close values and to fulfill the normalization condition

$$A^2 + B^2 = 1. \quad (3)$$

Considering that these two  $2^+$  states are simultaneously populated by direct and compound nucleus reaction mechanisms, we have developed formula (28) from reference [10], thus obtaining the following expression for the corresponding center of mass differential cross section.

$$\begin{aligned} \frac{d^2\sigma}{d\Omega dE}(\theta) = & \frac{N_d^2(\theta)(B+A)^2 + N_c^2(\theta)(C^2 + D^2)}{(E - E_1)^2 + \Gamma_1^2/4} + \frac{N_d^2(\theta)(B-A)^2 + N_c^2(\theta)(C^2 + D^2)}{(E - E_2)^2 + \Gamma_2^2/4} \\ & + 2N_d^2(\theta)(B+A)(B-A) \frac{(E - E_1)(E - E_2) + \Gamma_1\Gamma_2/4}{[(E - E_1)^2 + \Gamma_1^2/4][(E - E_2)^2 + \Gamma_2^2/4]}. \quad (4) \end{aligned}$$

In this expression, indices 1 and 2 refer, respectively, to the properties of the  $2^+$  (16.626) and  $2^+$  (16.922) states, the angle-dependent parts for the direct ( $d$ ) and compound nucleus

(*c*) contributions are contained, respectively, in the  $N_d(\theta)$  and  $N_c(\theta)$  terms, and C and D are the amplitudes of the compound nucleus states. Equation 4 then involves two Breit-Wigner shapes describing the two  $2^+$  states and their interference term. The nuclear level parameters entering in it were fitted using the CERN computer program PAW [39] to reproduce the experimental deuteron energy spectra. The fit parameters that had to be considered in this analysis were:  $E_1$ ,  $E_2 - E_1$ ,  $\Gamma_1$ ,  $\Gamma_2$ ,  $\alpha = N_d(\theta)(B + A)$ ,  $\beta = N_d(\theta)(B - A)$  and  $\gamma = N_c(\theta)(C^2 + D^2)$ . Then, this set of seven free physics parameters was further reduced to only four with adopting well established c. m. values of the level widths and resonance energies for the  $2^+$  isospin-mixed doublet from the literature [28], i.e., the  $\Gamma_1$ ,  $\Gamma_2$  and  $E_2 - E_1$  values reported in table I. The analysis of the deuteron energy spectra carried out using equation 4 has led us to a satisfactory reproduction of the shapes of the measured deuteron energy spectra. The corresponding fit parameters for the extracted direct reaction contribution in this equation are reported in table I (see the text below in this section). The spectrum recorded at  $\theta_{lab} = 35^\circ$ , showing the peaks associated with the two  $2^+$  states of  ${}^8\text{Be}$  well isolated and separated from each other, is reported in Fig. 2 where the solid curve represents the best fit to the experimental data points generated by the PAW software. As can be seen in this figure, the  $2^+(16.626)$  state is then much more populated than the  $2^+(16.922)$  upper state in the  ${}^7\text{Li}({}^3\text{He},d){}^8\text{Be}$  proton stripping reaction at bombarding energy,  $E_{lab} = 20$  MeV. Indeed, the ratio of the peak intensities (peak content areas) for these states,  $\frac{I_{16.626}}{I_{16.922}}$ , amounts here to 5.3 for  $\theta_{lab} = 35^\circ$  and increases with decreasing the observation angle (see Figs. (1, 2)). This behavior is consistent with the measurements of Piluso et al. on this transfer reaction at  $E_{lab} = 15$  MeV (see Fig. 3 of reference [29]), while at the lower  ${}^3\text{He}$  ion energy of  $\sim 11$  MeV the peaks associated with the two  $2^+$ , isospin-mixed states of  ${}^8\text{Be}$  were found to be of comparable heights and sizes (see references [10, 31]).

The quantities ( $A$ ,  $B$ ,  $\alpha$ ,  $\beta$ ) associated with the direct reaction component in equation 4 are related by

$$\frac{A}{B} = \frac{\alpha - \beta}{\alpha + \beta}. \quad (5)$$

Using this relation and the normalization condition of equation 3, one can deduce the values of coefficients  $A$ ,  $B$  and parameter  $N_d(\theta)$  for the direct reaction component. Then, values of the quantities  $A/B$ ,  $A + B$  and  $A - B$  have been obtained in the analysis of the different deuteron energy spectra recorded in this experiment. Averaging all  $A$  values, we derived the

	$E_2 - E_1$ (keV)	$\Gamma_1$ (keV)	$\Gamma_2$ (keV)	$\langle A \rangle$	$\langle B \rangle$	$\langle A/B \rangle$
This work	$296 \pm 6$	108.1	74.0	$0.797 \pm 0.036$	$0.604 \pm 0.08$	$1.32 \pm 0.08$
[10]	$274 + 3$	$113 \pm 3$	$73 \pm 3$	0.772	0.636	$1.47 \pm 0.07$

$\langle A \rangle$ ,  $\langle B \rangle$  and  $\langle A/B \rangle$  mean values listed in table I that show to be in fairly good agreement with the  $A$ ,  $B$  and  $A/B$  values obtained by Marion et al. [10] in their earlier study of the  ${}^7\text{Li}({}^3\text{He},d){}^8\text{Be}$  transfer reaction at  $E_{lab} \sim 11$  MeV. It therefore appears that the values of the ( $A$ ,  $B$ ) amplitudes associated with the direct reaction component in equation 4 are independent on the reaction bombarding energy.

Only parts of the peak areas of interest in the measured deuteron spectra due to the direct reaction component have been considered in our non local, FR-DWBA analysis (see Section III) of the measured  ${}^7\text{Li}({}^3\text{He},d){}^8\text{Be}$  angular distribution data. These peak areas were calculated using the relation

$$Area_i = \frac{2\pi H_i^2}{\Gamma_i} \quad (6)$$

where  $H_i = N_d(\theta)(A+B)$  or  $N_d(\theta)(A-B)$  depending on whether index  $i = 1$  or  $2$ , with  $N_d(\theta)$  denoting the angle-dependent part of the direct reaction component, as stated. Then, the derived count numbers for this component have been transformed into corresponding center of mass differential cross sections.

#### D. Experimental angular distributions

The derived angular distribution experimental data for the three states of  ${}^8\text{Be}$  studied here (i.e., the  $2^+(16.626)$ ,  $2^+(16.922)$  and  $1^+(17.64)$  excited states) are reported in Figs. (3, 4, 5). One can see that they exhibit marked forward peaking, as expected for direct proton transfer in the  ${}^7\text{Li}({}^3\text{He},d){}^8\text{Be}$  reaction at the considered high enough  ${}^3\text{He}^{2+}$  ion bombarding energy of 20 MeV. Notice that the first peak of the angular distributions for both three states is described experimentally for the first time in this work (compare to similar data from reference [30]). One can also observe in Figs. (3, 4) that the measured angular distributions for the  $2^+(16.626)$  and  $2^+(16.922)$  weakly bound states have qualitatively similar

shapes (although only deuteron forward angles are concerned here). Furthermore, for this  $2^+$  doublet of large isospin mixing the sets of experimental data contained in Figs. (1, 2, 3, 4) indicate that the lower state at 16.626 MeV is considerably more strongly populated than the upper state at 16.922 MeV. This observation is consistent with earlier assumptions [9] according to which these two  $2^+$  states are, respectively, characterized by the  ${}^7\text{Li}(\text{g.s.}) + \text{p}$  (i.e.,  $\alpha + \text{t} + \text{p}$ ) and  ${}^7\text{Be}(\text{g.s.}) + \text{n}$  (or  $\alpha + {}^3\text{He} + \text{n}$ ) single-particle model configurations. These properties have been largely confirmed since then in other previous works both experimentally and via theoretical (mainly shell-model) calculations. In particular, only the lower  $2^+(16.626)$  state was observed in the  ${}^7\text{Li}(\text{p},\gamma){}^8\text{Be}$  direct radiative proton capture [9] while the upper  $2^+(16.922)$  state was not populated in this reaction. In previous measurements of deuteron spectra from the  ${}^7\text{Li}({}^3\text{He},\text{d}){}^8\text{Be}$  reaction at  $E_{\text{lab}} = 10.972$  MeV [10] and 15 MeV [29], both two  $2^+$  isospin-mixed states have been observed to be comparably populated at  $\theta_{\text{lab}} = 40^\circ$  while at  $10^\circ$  and  $25^\circ$  the lower state at 16.626 MeV was found to be much more excited than the  $2^+(16.922)$  upper state. The ratio of the measured differential cross sections for these two states,  $\frac{(d\sigma/d\Omega)_{16.626}}{(d\sigma/d\Omega)_{16.922}}$ , was found to be an increasing function of the  ${}^3\text{He}$  ion bombarding energy. Its value derived in the current work is the highest one ever reported from the  ${}^7\text{Li}({}^3\text{He},\text{d}){}^8\text{Be}$  reaction. This ratio is higher at small detection angles attaining a maximum value of 58 for  $\theta_{\text{lab}} = 10^\circ$  while a minimum value of 9.7 is reached at  $\theta_{\text{lab}} = 30^\circ$ . This behavior was predictable because the proton stripping pattern of the  $2^+(16.626)$  state enhances its population at small forward angles. Notice that this ratio is considerably higher in comparison to the peak intensity ratio,  $\frac{I_{16.626}}{I_{16.922}}$ , reflecting the relative peak contents of the two  $2^+$ ,  $T = 0 + 1$  isospin-mixed states within the measured deuteron energy spectra. This is due to the two following facts:

(i) the differential cross section ratio corresponds here only to the direct reaction contribution in the  ${}^7\text{Li}({}^3\text{He}, \text{d}){}^8\text{Be}$  reaction; it then appears that the population of the  $2^+(16.922)$  upper state of dominant  ${}^7\text{Be} + \text{n}$  single-particle configuration by direct proton transfer is much less favourable than that of the  $2^+(16.626)$  lower state at the investigated  ${}^3\text{He}^{2+}$  ion energy of 20 MeV, while the population of both two states via the compound nucleus formation mechanism is expected to be drastically reduced,

ii) the interference between these two  $2^+$  states, which is indispensable for a correct treatment of the corresponding deuteron energy spectra, has been taken into account in the current study; its main effect is to enhance the ratio of the proton stripping yields to these

states as the bombarding energy increases (see reference [10]).

It was observed, indeed, that at  $^3\text{He}$  ion bombarding energies,  $E_{lab} = 11$  MeV (see reference [10]), 15 MeV (see reference [29]), 20 MeV (this experiment) and 33 MeV (see reference [30]), the  $^7\text{Li}(^3\text{He},d)^8\text{Be}$  reaction is increasingly dominated by the direct proton stripping mechanism essentially populating the  $2^+(16.626)$  state, while the  $2^+(16.922)$  state is much less favourably excited due to its characteristic  $^7\text{Be} + n$  configuration. As a result, the difference in peak heights for the two  $2^+$  states is considerably enhanced but the cross section ratio for the direct reaction component increases much more with bombarding energy than the peak intensity ratio for the two states. Then, the  $2^+(16.922)$  state has not been obviously pointed out in the deuteron spectra recorded by Basak et al. [30] in their study of the  $^7\text{Li}(^3\text{He},d)^8\text{Be}$  reaction for higher bombarding energy,  $E_{lab} = 33.3$  MeV; however, a corresponding shoulder can be seen in the high energy tail of the strong peak prominent in Fig. 1 (c) of reference [30], fully attributed by the authors to the  $2^+(16.626)$  state. Note also that the compound nucleus component (probably negligible, indeed, at this high ion bombarding energy) was not extracted by these authors. To our knowledge, no experimental angular distribution data for the weaker  $2^+(16.922)$  state of  $^8\text{Be}$  has been reported previously from the  $^7\text{Li}(^3\text{He},d)^8\text{Be}$  reaction. As stated in Section I, only a global experimental angular distribution exhibiting forward peaking has been reported [31] from this reaction for the  $2^+(16.626)$  state for  $E_{lab} = 10$  MeV, while the measured angular distribution for the  $2^+(16.922)$  state (not reported in reference [31]) was claimed to be roughly isotropic, very likely due to a significant compound nucleus contribution. In previous studies of other direct reactions involving  $^8\text{Be}$  as residual nucleus where the patterns of the  $2^+(16.626)$  and  $2^+(16.922)$  states were experimentally resolved, the corresponding angular distributions have been generally found to be also forward peaked and of similar shapes. This trend has been observed in the  $^{10}\text{B}(d,\alpha)^8\text{Be}$  reaction for 7.5 MeV incident deuterons [11] where a violation of the isospin selection rule was pointed out with a total cross section ratio,  $\frac{\sigma_{16.626}}{\sigma_{16.922}} = 1.15$ , determined without taking into account the interference between these two  $2^+$  states, whereas the latter states are expected to be equally populated in this  $T = 0$  reaction. Their trends versus bombarding energy was usually found to be consistent with Marion's single-particle model configuration assumptions [9]. That is, in reactions where the  $^7\text{Li} + p$  configuration is favoured, the  $2^+(16.626)$  state was observed to be typically much strongly populated relative to the weaker  $2^+(16.922)$  state. This was particularly the case in the  $^7\text{Li}(d,n)^8\text{Be}$  proton

stripping reaction (see reference [40] and references [1-6] therein). The measured neutron angular distributions from the latter reaction for high deuteron bombarding energy [41], never published in details, were found to have the following characteristics: (i) in the case of the  $2^+(16.922)$  state, the neutron angular distribution showed strong forward peaking consistently with a  $\ell = 1$  stripping scheme with a differential cross section value of about 23 mb/sr at  $\theta_{lab} = 0^\circ$ , (ii) that of the  $2^+(16.922)$  upper state was found to be essentially isotropic with an average cross section value of  $\sim 0.87$  mb/sr, hence a ratio  $\frac{(d\sigma/d\Omega)_{16.626}}{(d\sigma/d\Omega)_{16.922}} \simeq 26.44$ . The two members of the  $2^+$  isospin-mixed doublet of  $^8\text{Be}$  have also been pointed out in the  $^7\text{Li}(d, \alpha\alpha)n$  three-body breakup reaction [15, 42]. In the more recent of these studies carried out for deuteron energies in the range,  $E_{lab} = 3 - 6$  MeV [15] where the above two  $2^+$  states of the  $^8\text{Be}$  were experimentally well resolved, the measured coincidence spectra indicated strong direct proton population of the  $2^+(16.626)$  state at neutron emission forward angles consistently with the assumption [9] of predominant  $^7\text{Li}(\text{g.s.}) + p$  configuration for this state. In addition, the assumed interference between the two  $2^+$ , isospin-mixed states was confirmed experimentally in the latter work [15]. Besides, in a previous study of the  $^{11}\text{B}(p, \alpha)^8\text{Be}$  reaction at  $E_p = 40$  MeV [43] assumed to proceed via the knock out of an  $\alpha$ -particle from  $^{11}\text{B}$  leaving the  $^8\text{Be}$  nucleus in the  $^7\text{Li} + p$  (i.e.,  $\alpha + t + p$ ) configuration at this high proton energy, the angular distributions of both two  $2^+$ ,  $T = 0 + 1$  isospin-mixed states were found to be forward peaked and of nearly similar shapes with a 16.626/16.922 excitation energy ratio of  $2.3 \pm 0.4$ . Conversely, the  $2^+(16.922)$  state was observed to be more strongly populated in reactions favouring the  $^7\text{Be} + n$  single-particle model configuration, such as the  $^9\text{Be}(p, d)^8\text{Be}$  and  $^9\text{Be}(d, t)^8\text{Be}$  neutron pick-up reactions for high particle bombarding energies [44–46].

Finally, the experimental differential cross section for the formation of the  $^{10}\text{B}$  compound nucleus versus the observation angle proved to be not important in this  $^7\text{Li}(^3\text{He}, d)^8\text{Be}$  experiment at  $^3\text{He}^{2+}$  ion bombarding energy,  $E_{lab} = 20$  MeV. This component, likely originating only from the population of the  $2^+(16.922)$  weaker state, has been pointed out in the current analysis at only four detection angles. It has been evaluated within the  $^8\text{Be}$  excitation energy region,  $E_x = 16.626 - 16.922$  MeV, by inserting into equation 6 the parameter,  $\gamma = N_c(\theta)(C^2 + D^2)$ , for determining the corresponding number of counts in the deuteron energy spectra. It's observed shape was found to be roughly isotropic with average values of  $\sim 0.9, 0.4, 0.5$  and  $0.8$  mb/sr for  $\theta_{lab} = 25^\circ, 30^\circ, 35^\circ$  and  $40^\circ$ , respectively.

### III. ANALYSIS OF CROSS SECTION DATA, RESULTS AND DISCUSSION

#### A. FR-DWBA analysis of angular distribution data

The measured angular distributions for the two  $2^+$  bound states at  $E_x = 16.626$  and  $16.922$  MeV and the  $1^+$  unbound state at  $E_x = 17.640$  MeV of  ${}^8\text{Be}$  produced in the  ${}^7\text{Li}({}^3\text{He},d){}^8\text{Be}$  transfer reaction have been analyzed in terms of the Non Local, Finite Range-DWBA formalism for direct nuclear reactions [47] with focussing our attention essentially on the small deuteron forward angles. The calculations have been carried out using the computer code FRESKO [48] with assuming that the transfer of a proton occurs from the  ${}^3\text{He}^{2+}$  projectile onto the 1p-shell of the  ${}^7\text{Li}$  target nucleus. The optical model potential parameters adopted to describe the distorted waves in the  ${}^7\text{Li} + {}^3\text{He}$  entrance channel [49] and the  $d + {}^8\text{Be}$  exit channel [50] are reported in table II. The bound state wave functions were computed using Saxon-Woods potential form factors to describe the binding of the proton to the deuteron and  ${}^7\text{Li}$  cores in the entrance and exit channels, respectively, while the potential well depths for the  $p + d$  and  $p + {}^7\text{Li}$  systems have been adjusted to reproduce the corresponding experimental separation energies. For the  $1^+$  (17.640) unbound state, the DWBA cross sections were calculated by applying the procedure described in reference [51], in which the unbound state wave function is substituted by that of the  ${}^7\text{Li} + p$  system in a scattering resonance state. The resonance occurs at an energy for which the phase shift passes through  $\pi/2$  and the wave functions can be calculated by resolving the radial wave equation at the resonance energy. However, the oscillatory behavior of the final distorted wave and the unbound state wave functions induces convergence difficulties in the integral of the reaction matrix elements. FRESKO deals with unbound states by discretizing the continuum states in energy bins. A bin wave function is constructed by the superposition of scattering states within an energy range around the resonance energy. As the radial partial-wave integral converges very slowly, it must be extended over several hundreds of femtometers in order to obtain both the convergence and results independent on the upper value of the cutoff radius [52]. In the present case, we have used a value of 200 fm for this parameter.

Elastic scattering	$V_R$	$r_R$	$a_R$	$W_V$	$W_D$	$r_{V,D}$	$a_{V,D}$	$V_{s.o.}$	$r_{s.o.}$	$a_{s.o.}$	$r_c$
	(MeV)	(fm)	(fm)	(MeV)	(MeV)	(fm)	(fm)	(MeV)	(fm)	(fm)	(fm)
${}^3\text{He} + {}^7\text{Li}$ [49]	146.9	1.39	0.684	29.1	0	1.912	0.407	5.21	1.426	0.211	1.4
$d + {}^8\text{Be}$ [50]	90	0.9	0.9	10	6.25	1.6	0.8	5	1.6	0.8	1.3

## B. Results and discussion

### 1. Angular distributions

The DWBA-generated theoretical curves corresponding to best fits to the  ${}^7\text{Li}({}^3\text{He},d){}^8\text{Be}$  angular distribution experimental data for the three studied states of  ${}^8\text{Be}$  (the  $2^+(16.626)$  and  $2^+(16.922)$ ,  $T = 0 + 1$  isospin-mixed states and the  $1^+(17.64)$ ,  $T = 1$  state) are also plotted in Figs. (3, 4, 5). One observes that the cross section experimental data for the strongly populated  $2^+$  state at 16.626 MeV are satisfactorily reproduced by the DWBA-calculated curve, which further confirms the validity of the assumption [9] that the structure of this state is dominated by the  ${}^7\text{Li} + p$  single-particle model configuration. Those for the weaker  $2^+$  (16.922) state also appear to be well accounted for by our DWBA calculation. The good description by this theory of the angular distribution data from the  ${}^7\text{Li}({}^3\text{He},d){}^8\text{Be}$  proton stripping reaction for this state means that the structure of the latter also involves the  ${}^7\text{Li} + p$  single-particle model configuration and that it cannot be of pure  ${}^7\text{Be} + n$  configuration as assumed earlier in reference [9]. Therefore, by fitting the corresponding lowest forward angle cross section data, one can deduce a reliable proton spectroscopic information for this state from the  ${}^7\text{Li}({}^3\text{He},d){}^8\text{Be}$  proton stripping reaction at the relatively high  ${}^3\text{He}^{2+}$  ion bombarding energy of 20 MeV.

Besides, the angular distribution experimental data for the  $1^+(17.640)$  unbound state are less well reproduced by our DWBA calculation, as can be seen in Fig. 5. It must be noted that several theoretical fits to the angular distribution experimental data for this state have been tried without simultaneously accounting for all the measured cross section values. Finally, the following procedure was adopted : first, a theoretical best fit was obtained by considering all forward angle experimental data points; then, a second best fit was derived with ignoring the smallest angle data point that did not follow the calculated curve. Two corresponding  $C^2S$  values were thus determined and their mean value was



adopted. Consequently, a large uncertainty (standard deviation) of  $\sim 43\%$  has been assigned to the derived proton spectroscopic factors for this state.

## 2. Proton spectroscopic factors

The following expression relating the experimental differential cross section to the DWBA theoretical counterpart was used in order to deduce the proton spectroscopic factors for the three studied states of  ${}^8\text{Be}$

$$\left(\frac{d\sigma}{d\Omega}\right)_{\text{exp}} = 4.43C^2 \frac{2J_f + 1}{2J_i + 1} \sum_{n\ell j} \frac{S_{n\ell j}}{2j + 1} \left(\frac{d\sigma_{n\ell j}(\theta)}{d\Omega}\right)_{DWBA}. \quad (7)$$

In this formula, the factor of 4.43 is the commonly admitted value [53] to describe the  $\langle d \otimes p | {}^3\text{He} \rangle$  overlap function in the  $({}^3\text{He}, d)$  reaction, the  $C$  factor is the Clebsch-Gordon coefficient coupling the isospins of the target and final nuclei and the transferred particle (in the present case of the  ${}^7\text{Li}({}^3\text{He}, d){}^8\text{Be}$  reaction,  $C^2 = 1/2$  for the final states,  $T = 0, 1$ ),  $(J_i, J_f)$  are the respective spins of the target nucleus and the studied state in the residual nucleus, and  $S_{n\ell j}$  is the spectroscopic factor for the transfer of a proton onto a shell-model orbit of the  ${}^7\text{Li}$  target characterized by the  $\{n\ell j\}$  set of quantum numbers (i.e., the principal quantum number,  $n$ , the orbital and total angular momentum quantum numbers,  $\ell$  and  $j$ ) to form the final state of the  ${}^8\text{Be}$  nucleus. Due to their spin and parity characteristics,  $J_f^\pi = 2^+$  and  $1^+$ , the final states of  ${}^8\text{Be}$  considered in this study can be populated via both  $1p_{1/2}$  and  $1p_{3/2}$  captures. Then, for a dominating  $1p_{3/2}$  transition, equation 7 rewrites as

$$\left(\frac{d\sigma}{d\Omega}\right)_{\text{exp}} = 4.43C^2 \frac{2J_f + 1}{4(2J_i + 1)} \left\{ 1 + 2 \left( \frac{S_{1p_{1/2}}}{S_{1p_{3/2}}} \right) \frac{(d\sigma/d\Omega)_{1p_{1/2}}^{DWBA}}{(d\sigma/d\Omega)_{1p_{3/2}}^{DWBA}} \right\} S_{1p_{3/2}} \left(\frac{d\sigma}{d\Omega}\right)_{1p_{3/2}}^{DWBA}, \quad (8)$$

where  $S_{global}$  is defined as a global spectroscopic factor by

$$S_{global} = \left\{ 1 + 2 \left( \frac{S_{1p_{1/2}}}{S_{1p_{3/2}}} \right) \frac{(d\sigma/d\Omega)_{1p_{1/2}}^{DWBA}}{(d\sigma/d\Omega)_{1p_{3/2}}^{DWBA}} \right\} S_{1p_{3/2}}. \quad (9)$$

Since the shapes of the  $1p_{1/2}$  and  $1p_{3/2}$  capture cross sections calculated with the FRESCO program are quasi identical, their ratios in the latter equation have been considered as constants over the whole studied angular range,  $\theta_{lab} = 0^\circ - 50^\circ$ . The values of these ratios are reported in table III together with the  $S_{1p_{1/2}}/S_{1p_{3/2}}$  partial spectroscopic factor ratios derived

$J^\pi(E_x, MeV)$	T	$(d\sigma/d\Omega)_{1p_{1/2}}^{DWBA} / (d\sigma/d\Omega)_{1p_{3/2}}^{DWBA}$ This work	$(S_{1p_{1/2}}/S_{1p_{3/2}})_{C.K.}$ Cohen and Kurath [54]
$2^+(16.626)$	0 + 1	$0.660 \pm 0.034$	0.2262
$2^+(16.922)$	0 + 1	$0.680 \pm 0.043$	0.4190
$1^+(17.640)$	1	$1.036 \pm 0.019$	0.3857

here for the three studied states of  ${}^8\text{Be}$  based on Cohen and Kurath's shell model calculations [54] (see below). Indeed, neither the  $S_{1p_{1/2}}$  and  $S_{1p_{3/2}}$  partial spectroscopic factors nor their ratio,  $S_{1p_{1/2}}/S_{1p_{3/2}}$ , can be directly derived from the DWBA analysis. Fortunately, Cohen and Kurath have performed shell model calculations [54] where spectroscopic factors have been calculated for single nucleon stripping on the 1p shell of a target nucleus with mass number,  $A = 7$ , leading to the population of states with properties,  $J_f^\pi = 2^+$  ( $T = 0, 1$ ) and  $1^+$  ( $T = 1$ ), which we have identified to the  $2^+$  doublet at  $E_x = 16.626$  MeV and 16.922 MeV and the  $1^+$  state at  $E_x = 17.640$  MeV in  ${}^8\text{Be}$ , respectively. We have therefore used Cohen and Kurath's results to derive the  $S_{1p_{1/2}}/S_{1p_{3/2}}$  ratios reported in table III, that we have considered in equation 9 for deducing experimental values of the  $S_{1p_{1/2}}$  and  $S_{1p_{3/2}}$  partial spectroscopic factors for the 1p shell. Cohen and Kurath [54] have also calculated  $S_{1p_{1/2}}$  and  $S_{1p_{3/2}}$  spectroscopic factor values separately for each isospin state. Then, the  $(S_{1p_{1/2}}/S_{1p_{3/2}})_{C.K.}$  ratio following these authors [54] for the pure  $T = 1$  isospin state at 17.640 MeV was directly deduced, while the same ratio for the  $T = 0 + 1$  isospin-mixed states at 16.626 MeV and 16.922 MeV were derived using the spectroscopic factor values calculated as follows for  $j = 1/2$  and  $3/2$ :

$$\begin{aligned}
S_{1p_j \text{ C.K.}}(16.626 \text{ MeV}) &= AS_{1p_j \text{ C.K.}}(T = 0) + BS_{1p_j \text{ C.K.}}(T = 1), \\
S_{1p_j \text{ C.K.}}(16.922 \text{ MeV}) &= |BS_{1p_j \text{ C.K.}}(T = 0) - AS_{1p_j \text{ C.K.}}(T = 1)|,
\end{aligned}
\tag{10}$$

where  $A = 0.797$  and  $B = 0.604$  as defined in Section II.

The derived values of the absolute proton spectroscopic factor,  $C^2S_{global}$ , for the three studied states of  ${}^8\text{Be}$  are reported in table IV where they are compared to the only experimental values available in the literature deduced by Basak et al. [30] from the  ${}^7\text{Li}(\overrightarrow{{}^3\text{He}}$ ,

$J^\pi(E_x, \text{MeV})$	$C^2S_{global}$ results			
	This work	Basak [30]	Cohen and Kurath [54]	F. C. Barker [13]
$2^+(16.626)$	$0.650 \pm 0.097$	$1.05 \pm 0.10$	0.775	0.475
$2^+(16.922)$	$0.0195 \pm 0.007$	$a$	0.071	0.005
$1^+(17.640)$	$0.439 \pm 0.190$	$0.30 \pm 0.15$	0.289	$0.145^b$

<sup>a</sup>Unseparated from the 16.626 MeV state.

<sup>b</sup>From resonance reaction

d)<sup>8</sup>Be transfer reaction for a bombarding energy,  $E_{lab} = 33.3$  MeV. We recall here that probably due to insufficient experimental energy resolution, the peaks for the  $2^+$  (16.626) and  $2^+$  (16.922) states in the deuteron energy spectra from that experiment [30] were not separated. Furthermore, considering the latter state to be of pure  ${}^7\text{Be} + n$  single-particle model configuration, these authors have neglected its weak excitation in the  ${}^7\text{Li}(\overrightarrow{{}^3\text{He}}, d){}^8\text{Be}$  reaction and, then, have likely over-estimated the population of the stronger  $2^+$  (16.626) state in this reaction, which could explain why their extracted  $C^2S_{global}$  value is a factor 1.61 times our result.

In order to compare our experimental  $C^2S_{global}$  values to corresponding theoretical counterparts, we have used equation 9 with the spectroscopic factor values calculated by Cohen and Kurath [54]. These authors obtained the following global spectroscopic factors for each isospin  $T$ - value: 0.289 ( $J^\pi = 1^+, T = 1$ ), 0.575 ( $J^\pi = 2^+, T = 0$ ) and 0.525 ( $J^\pi = 2^+, T = 1$ ). Then, the Cohen and Kurath  $C^2S_{global}$  values reported in table IV for the  $T = 0 + 1$  isospin - mixed states have been calculated using the relations

$$\begin{aligned}
C^2S_{global \ C.K.}(16.626 \text{ MeV}) &= AC^2S_{global \ C.K.}(T = 0) + BC^2S_{global \ C.K.}(T = 1), \quad (11) \\
C^2S_{global \ C.K.}(16.922 \text{ MeV}) &= |BC^2S_{global \ C.K.}(T = 0) - AC^2S_{global \ C.K.}(T = 1)|.
\end{aligned}$$

Besides, the results derived here for the proton ( $S_{1p_{1/2}}, S_{1p_{3/2}}$ ) partial spectroscopic factors of the three studied states of <sup>8</sup>Be are reported in table V where they are compared to Cohen and Kurath's shell model predictions [54].

One can observe, first, in both two tables (IV, V) that our spectroscopic factors for the

weakly excited  $2^+(16.922)$  state are remarkably smaller than those for the strongly populated  $2^+(16.626)$  state in the  ${}^7\text{Li}({}^3\text{He},d){}^8\text{Be}$  reaction, in overall consistency with shell model predictions [13, 54]. These results, which can be expected from the corresponding patterns of these two  $2^+$  states in the recorded deuteron energy spectra (see Figs. (1, 2)) and from the measured angular distributions (see Figs. (3, 4)) obviously confirm Marion's assumptions [9, 10] that the  ${}^7\text{Be} + n$  and  ${}^7\text{Li} + p$  single-particle model configurations dominate, respectively, the structures of these two  $2^+$ ,  $T = 0 + 1$  isospin-mixed states. As can be seen in table IV, our new  $C^2S_{global}$  experimental value for the strongly excited  $2^+$  (16.626) state is in good agreement with Cohen and Kurath's [54] shell model-predicted one. It is also very consistent with the value derived by Barker [13] who has performed shell model calculations for  ${}^8\text{Be}$  states using single-particle wave functions in a harmonic oscillator potential. Concerning the  $S_{1p_{1/2}}$  and  $S_{1p_{3/2}}$  partial spectroscopic factors (see table V), a similar agreement is also observed between our values for the  $2^+$  (16.626) state and corresponding Cohen and Kurath's shell-model-predicted ones [54]. In the case of the  $2^+(16.922)$  weaker state, however, our results are substantially lower than the predictions of Cohen and Kurath: by a factor of  $\sim 3.64$  concerning  $C^2S_{global}$  (see table IV) and by more than one order of magnitude concerning the  $S_{1p_{1/2}}$  and  $S_{1p_{3/2}}$  partial spectroscopic factors (see table V). Note that, in contrast, our experimental value of  $C^2S_{global}$  for this state (see table IV) is a factor 3.9 higher than that derived by Barker via shell model calculation [13].

It is thus clearly pointed out here that the population of the  $2^+(16.922)$  state in the  ${}^7\text{Be} + n$  single-particle model configuration is minor in the  ${}^7\text{Li}({}^3\text{He},d){}^8\text{Be}$  proton stripping reaction. Cohen and Kurath's effective-interaction calculations [54] are charge independent. Then, the corresponding shell model spectroscopic factors for the  $2^+(16.922)$  state should be more appropriately compared to experimental counterparts resulting from a DWBA analysis of angular distribution data for neutron transfer reactions populating this state in its dominant  ${}^7\text{Be} + n$  configuration, like the  ${}^7\text{Be}(d,p){}^8\text{Be}$  and  ${}^7\text{Be}(t,d){}^8\text{Be}$  stripping reactions or the  ${}^9\text{Be}(p,d){}^8\text{Be}$  and  ${}^9\text{Be}(d,t){}^8\text{Be}$  pick-up reactions. Indeed, absolute neutron  $C^2S$  values derived for the latter state from the  ${}^7\text{Be}(d,p){}^8\text{Be}$  and  ${}^9\text{Be}(d,t){}^8\text{Be}$  reactions can be found in references [45, 46], respectively, where they are compared to experimental values from earlier works and to Cohen and Kurath's shell-model predictions [54].

$J^\pi(E_x, MeV)$	This work		Cohen and Kurath [54]	
	$S_{1p_{1/2}}$	$S_{1p_{3/2}}$	$S_{1p_{1/2}}$	$S_{1p_{3/2}}$
$2^+(16.626)$	$0.226 \pm 0.041$	$1.001 \pm 0.184$	0.270	1.194
$2^+(16.922)$	$0.010 \pm 0.001$	$0.025 \pm 0.003$	0.134	0.321
$1^+(17.640)$	$0.188 \pm 0.085$	$0.488 \pm 0.222$	0.124	0.321

Concerning the  $1^+(17.640)$ ,  $T = 1$  state of  ${}^8\text{Be}$ , one can observe in tables (IV, V) that the proton  $C^2S_{global}$  and  $(S_{1p_{1/2}}, S_{1p_{3/2}})$  values derived in this work are very consistent both with the experimental value of Basak et al. [30] and with Cohen and Kurath's [54] shell model predictions with all results being comprised within the experimental error bars. One must note, in passing, the observed very good agreement between the  $C^2S_{global}$  value derived for this state by Basak et al. [30] and the shell model-predicted value of Cohen and Kurath [54]. The present DWBA proton spectroscopic factor results for the  $2^+$ ,  $T = 0 + 1$  isospin-mixed doublet in  ${}^8\text{Be}$  appear to be essentially new since while no previous  $C^2S_{global}$  experimental value from the  ${}^7\text{Li}({}^3\text{He}, d){}^8\text{Be}$  transfer reaction has been reported in the literature for the weaker  $2^+(16.922)$  state, the unique value derived by Basak et al. [30] for the  $2^+(16.626)$  strongly excited state is not well consistent with shell model predictions [13, 54]. Note, in addition, that no experimental data from this reaction do exist in the previous literature concerning the proton  $S_{1p_{1/2}}$  and  $S_{1p_{3/2}}$  partial spectroscopic factors for both three states of  ${}^8\text{Be}$  considered in this study.

### 3. $\gamma_p^2(a)$ proton reduced widths

With the knowledge of the proton spectroscopic factors inferred in our DWBA analysis, the proton reduced widths versus the  $p+{}^7\text{Li}$  system channel radius can be derived from basic nuclear physics relations. For this purpose, the used expression was that defined in [55, 56], summed over the  $1p_{1/2}$  and  $1p_{3/2}$  proton capture shells of  ${}^8\text{Be}$  in terms of the individual spectroscopic factors, i.e.,

$$\gamma_p^2(a) = \frac{\hbar^2}{2\mu a} \left[ S_{1p_{1/2}} \left| u_{1p_{1/2}}(a) \right|^2 + S_{1p_{3/2}} \left| u_{1p_{3/2}}(a) \right|^2 \right], \quad (12)$$

where  $\mu$  is the reduced mass of the  $p+{}^7\text{Li}$  system and  $u_{n\ell j}(a)$  is the relative motion radial wave function calculated at channel radius

$$a = a_0 (A_p^{1/3} + A_{7Li}^{1/3}). \quad (13)$$

The obtained  $\gamma_p^2(a)$  values for the three studied states of  ${}^8\text{Be}$  at 16.626, 16.922 and 17.640 MeV excitation energies are reported in table VI where they are compared to counterparts reported by Barker from an R-Matrix analysis [34] of improved (ancient) cross section experimental data for the  ${}^7\text{Li}(p,\alpha){}^4\text{He}$  reaction (for the  $2^+(16.626)$  state) or following shell model calculations (for the  $2^+(16.922)$  state [34] and the  $1^+(17.640)$  state [14]). Notice, first, that for each of the three studied states of  ${}^8\text{Be}$ , notably the  $1^+(17.640)$  state, our derived DWBA proton reduced widths versus the channel radius,  $\gamma_p^2(a)$ , approximately remain in the same order of magnitude and that they are consistent with Barker's shell model or R-Matrix analysis derived values [14, 34] (see table VI). As can be seen in this table, the  $\gamma_p^2(a)$  values derived here for the strongly populated  $2^+(16.626)$  state in the  ${}^7\text{Li}({}^3\text{He},d){}^8\text{Be}$  proton stripping reaction are higher by more than one order of magnitude (precisely by factors of 35.25, 34.48 and 34.17, respectively for  $a = 3.64, 4.22$  and  $5.00$  fm) than those obtained for the weaker  $2^+(16.922)$  excited state. Again, this observation reflects the fact that the structures of these two  $2^+, T = 0 + 1$  isospin-mixed states of  ${}^8\text{Be}$  are indeed respectively dominated by the  ${}^7\text{Li} + p$  and  ${}^7\text{Be} + n$  single-particle model configurations [9, 10]. Comparatively, the corresponding  $\gamma_p^2(a)$  values reported by Barker [34] from R-Matrix analysis (for the  $2^+(16.626)$  state) or shell model calculation (for the  $2^+(16.922)$  state) are within a ratio of 60. Performing later an R-Matrix analysis of more recent experimental data for the  ${}^7\text{Li}(p,\alpha){}^4\text{He}$  reaction, Barker [57] has obtained a  $\gamma_p^2$  value for the  $2^+(16.626)$  state in agreement with our corresponding DWBA result but his derived  $\gamma_p^2$  value for the  $2^+(16.922)$  state substantially differs from our DWBA counterpart (see column 7 of table VI for channel radius,  $a = 4.22$  fm). The  $\gamma_p(a)$  proton reduced width amplitudes or the related  $\Gamma_p$  proton partial widths are commonly used as free fit parameters in this type of theoretical analysis [34, 57]. In the case of unbound states, the proton partial width expresses as

$$\Gamma_p = 2P_\ell(E) \times \gamma_p^2, \quad (14)$$

where  $P_\ell(E)$  is the Coulomb barrier penetration factor for the involved  $\ell$ - partial wave. However, for sub-threshold states (here the  $2^+$  doublet of  ${}^8\text{Be}$ ),  $P_\ell(E)$  cannot be calculated at the corresponding negative resonance energies, and  $\Gamma_p$  can be only estimated via several approximate methods, usually in terms of the proton spectroscopic factor times a single-

$\gamma_p^2$ (MeV)						
Present work				Ref.[14]	Ref. [34]	Ref. [57]
	$a = 3.64$ fm	$a = 4.22$ fm	$a = 5.00$ fm	$a = 4.22$ fm		
$2^+(16.626)$	2.08	1.54	0.991		0.896	1.659
$2^+(16.922)$	0.059	0.046	0.029		0.015	0.213
$1^+(17.640)$	1.4	0.95	0.284	0.321		

particle model proton width (see [58] and references therein). The derived values of  $\gamma_p^2$  (then of  $\gamma_p$  and  $\Gamma_p$ ) generally depend on the adopted reaction channel radius and can be also sensitive to the experimental data sets considered in the R-Matrix analysis [34, 57] for fixed value of  $a$ . Besides, one can observe in table VI that our DWBA-derived values of  $\gamma_p^2(a)$  for the  $2^+(16.626)$  strongly excited state in the  ${}^7\text{Li}({}^3\text{He},d){}^8\text{Be}$  proton stripping reaction show to be higher than those for the  $1^+(17.640)$  state by factors of only 1.49, 1.62 and 3.49 for  $a = 3.64$ , 4.22 and 5.00 fm, respectively, which is an indication that the structure of the latter narrow  $T = 1$  state appears to be substantially featured by the  ${}^7\text{Li} + p$  single-particle model configuration, consistently with Marion’s earlier assumption [40]. Finally, our  $\gamma_p^2(a)$  results for the three studied states of  ${}^8\text{Be}$  are indeed very concordant with previous observations, as reported in reference [40].

As stated in Section I, our DWBA proton reduced widths could be very useful for quantifying the contributions of the studied  ${}^8\text{Be}$  states in various nuclear physics or nuclear astrophysics topics via interaction processes involving this nucleus. In this respect, a careful, new and thorough R-Matrix analysis of up-dated, appropriately normalised angular distribution and integrated cross section experimental data sets available in the literature both via direct [33, 59, 60] and indirect [61–63] measurement methods for the  ${}^7\text{Li}(p,\alpha){}^4\text{He}$  hydrogen burning reaction of main astrophysical concern with considering the current DWBA results appears to us as highly desirable.

#### IV. SUMMARY AND CONCLUSIONS

In this work, a complete and up-to-date status of the spectroscopic properties of the  $^8\text{Be}$   $2^+$  (16.626) and  $2^+$  (16.922),  $T = 0 + 1$  isospin-mixed state of crucial interest in nuclear astrophysics has been addressed for several purposes, mainly regarding the nucleosynthesis of  $^7\text{Li}$  [17]. In this respect, we have measured the corresponding angular distributions in the  $^7\text{Li}(^3\text{He},d)^8\text{Be}$  transfer reaction for  $^3\text{He}^{2+}$  ion bombarding energy,  $E_{lab} = 20$  MeV, covering the forward angular range,  $5^\circ \leq \theta_{lab} \leq 50^\circ$ , in  $5^\circ$  steps. A clear separation in the recorded deuteron energy spectra of the peaks associated with these two  $2^+$  states has been achieved, thanks to the high energy resolution of the detection system used in the experiment. As expected, the  $2^+$  (16.626) state, essentially featured by the  $^7\text{Li} + p$  single-particle model configuration [9, 10], showed to be much more strongly populated than the  $2^+$  (16.922) state confirmed to be primarily of the  $^7\text{Be} + n$  configuration, pointed out here to be minor in this reaction for the considered kinematics. In addition, the angular distribution for the narrow  $1^+$ (17.640),  $T = 1$  state was measured. The experimental data for the above three states of  $^8\text{Be}$  have been analysed in the framework of the non-local, FR-DWBA theory by considering proton captures from the  $^3\text{He}^{2+}$  projectiles onto the  $1p_{3/2}$  and  $1p_{1/2}$  shells of the final nuclei. Updated values of the proton absolute and partial spectroscopic factors as well as of the proton reduced widths have been extracted for these three states. Within the DWBA uncertainties, our  $C^2S_{global}$  value for the  $2^+$  (16.626) strongly excited state was found to be in good agreement with shell-model predictions [13, 54], while the unique previous experimental value for this state (see reference [30]) was found to exceed our result by  $\sim 40\%$  and to lie substantially above theoretical predictions. In contrast, our  $C^2S_{global}$  result for the  $2^+$ (16.922) weakly populated state was found to be lower by a factor of  $\sim 3.64$  than Cohen and Kurath's [54] shell model value and in excess by a factor of 3.9 relative to Barker's [13] theoretical value. Similar observations evenly hold concerning the derived ( $S_{1p_{1/2}}$ ,  $S_{1p_{3/2}}$ ) partial spectroscopic factors for the three studied states, i.e., fair agreement between our DWBA values for the  $2^+$ (16.626) and  $1^+$ (17.640) states and their corresponding shell model counterparts [54], and large differences concerning the  $2^+$ (16.922) state of predominant  $^7\text{Be} + n$  single-particle model configuration. Besides, the  $\gamma_p^2(a)$  proton reduced widths versus the  $^7\text{Li} + p$  channel radius have been deduced from our DWBA analysis of the experimental angular distribution data. The derived values for a  $^7\text{Li} + p$  channel radius,  $a = 4.22$  fm,



were found to be consistent both with earlier shell model calculations for the  $2^+(16.922)$  state [34] and the  $1^+(17.640)$  state [14], and in good agreement for the  $2^+(16.626)$  state with a counterpart value derived by Barker [57] from an R-Matrix analysis of more recent experimental data for the  ${}^7\text{Li}(p,\alpha){}^4\text{He}$  resonant reaction of astrophysical concern. Then, the  $\gamma_p(a)$  reduced width amplitudes (or the related  $\Gamma_p(a)$  proton partial widths) can be used in the R-Matrix analysis of cross section experimental data for this reaction. The present DWBA results concerning the spectroscopic parameters of the three studied excited states of  ${}^8\text{Be}$  could be further confirmed via a similar study of the  ${}^7\text{Li}(d,n){}^8\text{Be}$  proton stripping reaction for which cross section angular distribution data for high deuteron bombarding energy are very lacking in the literature. In addition, the measurement of the angular distributions for the  ${}^7\text{Li}({}^3\text{He},d){}^8\text{Be}$  transfer reaction at  ${}^3\text{He}$  ion bombarding energy,  $E_{lab} = 33$  MeV, could permit to compare in the same kinematics conditions the obtained results to those of Basak et al. [30], and also to check if the  $(A, B)$  amplitudes of the direct reaction component in equation 4 are completely independent on the reaction bombarding energy. The DWBA results inferred here can be pertinently used to address several open questions in nuclear physics and nuclear astrophysics concerning interaction processes involving the  ${}^7\text{Li}$  and/or  ${}^8\text{Be}$  isotopes, as emphasised in Section I. In particular, a new R-Matrix analysis of relevant, well selected and appropriately normalised cross section experimental data for the  ${}^7\text{Li}(p,\alpha){}^4\text{He}$  hydrogen burning reaction with considering the present  $\gamma_p(a)$  DWBA-extracted results appeared to us as highly necessary, and has been recently undertaken by members [64] of our group. Thanks to the R-Matrix analyses of the available large corpus of precise experimental data sets accumulated during the last four decades for the  ${}^7\text{Li}(p,\alpha){}^4\text{He}$  reaction (involved in BBN and stellar nucleosyntheses) both via direct and indirect measurement methods, the associated astrophysical  $S(E)$ -factor and  $N_A \langle \sigma v \rangle$  rate can be determined with very high accuracy at thermonuclear energies. The corresponding results can be very helpful to obtain reliable informations on the abundance of lithium and beryllium isotopes in different astrophysical sites. On the other hand, these results strongly support existing clear experimental evidences for  $({}^8\text{Be})$  compound nucleus formation in the  ${}^7\text{Li}(p,\alpha){}^4\text{He}$  fusion reaction at thermonuclear energies, in contrast with previous indications [32] according to which a three-nucleon transfer reaction mechanism would dominate the proton sub-Coulomb energy regime of this reaction.

#### ACKNOWLEDGMENTS :

One of us (S. O.) is indebted to Dr A. Coc from the CSNSM/Orsay for helpful discussion, and to Prof M. Debiane from the USTHB/Algiers for providing some bibliography items.

---

- [1] S. Ouichaoui, H. Beaumevieille, N. Bendjaballah and A. Genoux-Lubain, *Il Nuovo Cimento* **94** A, N.2, 133 (1986); S. Ouichaoui, H. Beaumevieille, N. Bendjaballah, C. Chami, A. Dauchy, B. Chambon, D. Drain and C. Pastor, *Il Nuovo Cimento* **86** A, N.2, 170 (1985).
- [2] J. Carlson, S. Gandolfi, F. Pederiva, Steven C. Pieper, R. Schiavilla, K. E. Schmidt, and R. B. Wiringa, *Rev. Mod. Phys.* **87**, 1067 (2015); A. Fritsch, S. Beceiro-Novo, D. Suzuki, W. Mittig, J. J. Kolata, T. Ahn, D. Bazin, F. D. Becchetti, B. Bucher, Z. Chajecski, X. Fang, M. Febbraro, A. M. Howard, Y. Kanada-En'yo, W. G. Lynch, A. J. Mitchell, M. Ojaruega, A. M. Rogers, A. Shore, T. Suhara, X. D. Tang, R. Torres-Isea, and H. Wang, *Phys. Rev. C* **93**, 014321 (2016).
- [3] P. von Brentano and M. Philipp, *Phys. Lett. B* **454**, 171 (1999); P. von Brentano, *Phys. Rep.* **264**, 57 (1996); E. Hernandez and M. Mondragon, *Phys. Lett. B* **326**, 1 (1994); W. Von Oertzen, Martin Freer, Yoshiko Kanada-En'yod, *Phys. Rep.* **432**, 43 (2006); M. Freer, *Prog. Phys.* **70**, 2149 (2007).
- [4] D. D. Warner, M. A. Bentley and P. Van Isacker, *Nature Physics* **2**, 311 (2006); B. Blank and M.J.G. Borge, *Progress in Particle and Nucl. Phys.* **60**, 403 (2008); E. G. Lanz, A. Vitturi, M. V. Andrés, F. Catar and D. Gambacurt, *Phys. Rev. C* **84**, 064602 (2011).
- [5] David Jenkins, *J. Phys. G. : Nucl. Part. Phys.* **43**, 024003 (2016). Proceedings of the 7th International Conference on Clustering Aspects of Nuclear structure and Dynamics, Rab, Island of Croatia, 14-19 June 1999, Edited by M. Korolija, Z. Basrak, R. Caplar (World Scientific, 2000), p. 454. C. Beck, *Clusters in Nuclei, Vol 1–3 (Lecture Notes in Physics, Vol 875)* (Berlin: Springer, 2014).
- [6] E.G. Adelberger et al., *Rev. Mod. Phys.* **70**, 1265 (1998); T. Kajino and R.N. Boyd, *Astrophys. J.* **359**, 267 (1990); J.N. Bahcall and M.H. Pinsonneault, *Rev. Mod. Phys.* **64**, 885 (1992); D.N. Schramm and M.S. Turner, *Ibid.* **70**, 303 (1998).
- [7] G. Steigman, *Ann. Rev. Nucl. Part. Sci.* **29**, 313 (1979); G. Steigman, *Ann. Rev. Nucl.Part. Sci.* **57**, 463 (2007).
- [8] F. Iocco et al., *Phys. Rep.* **472**, 1 (2009).

- [9] M. Wilson and J. B. Marion, *Phys. Lett.* **14**, 313 (1965); J. B. Marion and M. Wilson, *Nucl. Phys.* **77**, 129 (1966).
- [10] J. B. Marion, P. H. Nettles, C. L. Cocke and G. J. Stephenson, Jr., *Phys. Rev.* **157**, 847 (1967).
- [11] C. P. Browne and J. R. Erskine, *Phys. Rev.* **143**, 683 (1966).
- [12] F. C. Barker, *Aust. J. Phys.* **31**, 27 (1978).
- [13] F. C. Barker, *Nucl. Phys.* **83**, 418 (1966).
- [14] F. C. Barker, *Aust. J. Phys.* **49**, 1081 (1996).
- [15] N. Godinovic', S. Blagus, M. Bogovac, M. Lattuada, M. Milin, D. Miljanic', D. Rendic', N. Soic', C. Spitaleri, and M. Zadro, *Phys. Rev. C* **60**, 037601 (1999).
- [16] C. A. Bertulani, Shubhchintak, A. Mukhamedzhanov, A. S. Kadyrov, A. Kruppad, and D. Y. Pang, 8th European Summer School on Experimental Nuclear Astrophysics (Santa Tecla School) IOP Publishing, *Journal of Physics: Conference Series* **703**, 012007 (2016); A. Coc, F. Hammache and J. Kiener, *Eur. Phys. J. A* **51**, 34(2015).
- [17] C. A. Bertulani and T. Kajino, *Prog. Part. Nucl. Phys.* **89**, 56 (2016); C. Brogini, L. Canton, G. Fiorentini, F. L. Villante, *J. Cosmol. Astropart. Phys.* **06**, 30 (2012); B. D. Fields, The primordial lithium problem, *Annu. Rev. Nucl. Part. Sci.* **61**, 47 (2011).
- [18] R. G. Pizzone, R. Sparta, C. Bertulani, C. Spitaleri, M. La Cognata, J. Lalmansingh, L. Lamia, A. Mukhamedzhanov, A. Tumino, *Astrophys. J.* **786**, 112 (2014).
- [19] Richard H. Cyburt, Brian D. Fields, Keith A. Olive, Tsung-Han Yeh, *Rev. Mod. Phys.* **88**, 015004 (2016).
- [20] M. Asplund, D. L. Lambert, P. E. Nissen, F. Primas, V. V. Smith, *Astrophys. J.* **644**, 229 (2006).
- [21] A. Coc, J.-P. Uzan, E. Vangioni, *J. Cosm. Astropart. Phys.* **10**, 50 (2014).
- [22] M. Anders, et al., *Phys. Rev. Lett.* **113**, 042501 (2014).
- [23] Mukhamedzhanov, Shubhchintak and C. A. Bertulani, *Phys. Rev. C* **93**, 045805 (2016)
- [24] A. Coc, *Proc. 14th Int. Symp. on Nuclei in the Cosmos (NIC2016)*, *JPS Conf. Proc.*, 010102 (2017), <https://doi.org/10.7566/JPSCP.14.010102>
- [25] A. J. Krasznahorkay et al., *Phys. Rev. Lett.* **116**, 042501 (2016).
- [26] A. Goudelis, M. Pospelov, and J. Pradler, *Phys. Rev. Lett.* **116**, 211303 (2016); J. L. Feng, B. Fornal, I. Galon, S. Gardner, J. Smolinsky, T. M. P. Tait, and P. Tanedo, *Phys. Rev. Lett.*

- 117, 071803 (2016); Phys. Rev. D **95**, 035017 (2017).
- [27] D. F. Jackson, Nuclear Reactions, Methuen and Co Ltd, London, 1970.
- [28] F. Ajzenberg-Selove, Nucl. Phys. A **490**, 1 (1988); F. Ajzenberg-Selove, Nucl. Phys. A **413**, 1 (1984); D.R. Tilley et al., Nucl. Phys. A **745**, 155 (2004).
- [29] C. J. Piluso, R. H. Spear, K. W. Carter, D. C. Kean and F. C. Barker, Aust. J. Phys. **24**, 459 (1971).
- [30] A. K. Basak, O. Karban, S. Roman, G. C. Morrison, C. O. Blyth, and J. M. Nelson, Nucl. Phys. A **368**, 93 (1981).
- [31] C. L. Cocke, Nucl. Phys. A **110**, 321 (1968).
- [32] G. Raimann et al., Phys. Lett. B **249**, 191 (1990).
- [33] S. Engstler et al., Z. Phys. **342**, 471 (1992).
- [34] F. C. Barker, Astrophys. J. **173**, 477 (1972).
- [35] A. Belhout et al., Nucl. Phys. A **793**, 178 (2007).
- [36] H. A. Enge, Nucl. Instrum. Methods. **28**, 119 (1964); J. Spencer and H. A. Enge, Nucl. Instrum. Methods. **49**, 181 (1967).
- [37] G. Rotbard, G. Berrier-Ronsin, O. Constantinescu, S. Fortier, S. Gales, M. Hussonnois, J.B. Kim, J.M. Maison, L.H. Rosier, J. Vernotte, C. Briancon, R. Kulesa, Y.T. Oganessian and S.A. Karamian, Phys. Rev. C **48**, R2148 (1993).
- [38] J. Vernotte, G. Berrier-Ronsin, J. Kalifa, and R. Tamisier, Nucl. Phys. A **390**, 285 (1982).
- [39] René Brun, Olivier Couet, Carlo E. Vandoni and Pietro Zanarini, Computer Physics Communications, **57**, 432 (1989).
- [40] J. B. Marion, Nucl. Phys. **68**, 463 (1965).
- [41] F. S. Dietrich and L. Cranberg, Bull. Am. Phys. Soc. **5**, 493 (1960); R.G. Kerr, *ibid.* **12**, 33 (1967); F.S. Dietrich and C. D. Zafiratos, *ibid.* **10**, 439 (1995).
- [42] V. Valkovic', W. R. Jacson, Y. S. shen, S. T. Emerson and G. C. Phillips, Nucl. Phys. A **96**, 241 (1967); R.E. Warner, B.A. Vaughan, J. A. DiTusa, J. W. Rovine, R. S. Wakeland, C. P. Browne, S. E. Darden, S. Sen, A. Nadasen, A. Basek, T.R. Donoghue, T. Rinckel, K. Sale, G. C. Ball, W. G. Davies, A. J. Ferguson, and J. S. Forster, Nucl. Phys. A **470**, 339 (1987).
- [43] D. G. Kamke and C. D. Goudman, Nucl. Phys. A **172**, 555 (1971).
- [44] J. B. Marion, C. A. Ludemann and P. G. Roos, Phys. Lett. **22**, 172 (1966); J. K. P. Lee, S. K. Mark, P. M. Portner and R. B. Moore, Nucl. Phys. A **106**, 357 (1968).

- [45] L. A. Kull, Phys. Rev. **163**, 1066 (1967); J. L. Schoonover, T. Y. Li and S. K. Mark, Nucl. Phys. A **176**, 567 (1971).
- [46] M. A. Oothoudt and G. T. Garvey, Nucl. Phys. A **284**, 41 (1977).
- [47] M. A. Preston, Physics of the Nucleus, Addison-Wesley, Reading, Massachusetts (1962).
- [48] I. J. Thompson, Comput. Phys. Rep. **7**, 167 (1988).
- [49] A. K. Basak, O. Karban, S. Roman, G. C. Morrison, C. O. Blyth, and J. M. Nelson, Nucl. Phys. A **368**, 74 (1981).
- [50] R. L. Dixon and R.D. Edge, Nucl. Phys. A **156**, 33 (1967).
- [51] Joaquín Gómez Camacho and Antonio M. Moro, The Euroschool on Exotic Beams, Vol. IV, Volume 879 of the series Lecture Notes in Physics pp 39-66.
- [52] H. T. Fortune, J. T. Gray, W. Trost, and N. R. Fletcher, Phys. Rev. **179**, 1033 (1969).
- [53] R. H. Bassel, Phys. Rev. **149**, 791 (1993).
- [54] S. Cohen and D. Kurath, Nucl. Phys. A **101**, 1 (1967).
- [55] A. M. Lane and R. G. Thomas, Rev. Mod. Phys. **30**, 257 (1958).
- [56] J. M. Blatt and V. F. Weisskopf, Theoretical Nuclear Physics (John Wiley & Sons, New York, 1952) p. 420; A. G. Sitenko, Theory of Nuclear Reactions (World Scientific, Singapore, 1990) p. 137.
- [57] F. C. Barker, Phys. Rev. C **62**, 044607 (2000).
- [58] C. Iliadis, Nuclear Physics A **618**, 166 (1997).
- [59] C. Rolfs and R. W. Kavanagh, Nucl. Phys. A **455**, 179 (1986).
- [60] J. Cruz et al., Phys. Lett. B **624**, 181 (2005); J. Cruz et al., J. Phys. G **35**, 014004 (2008).
- [61] C. Spitaleri, M. Aliotta, S. Cherubini, M. Lattuada, Dj. Miljanic', S. Romano, N. Soic, M. Zadro, and R. A. Zappala', Phys. Rev. C **60**, 055802 (1999); M. Lattuada et al., Astron. Astrophys. **562**, 1076 (2001).
- [62] R. G. Pizzone et al., Astron. Astrophys. **398**, 423 (2003).
- [63] L. Lamia, C. Spitaleri, M. La Cognata, S. Palmerini, and R. G. Pizzone, Astron. Astrophys. **541**, A158 (2012).
- [64] S. Ouichaoui et al., to be published.

**Tables captions:**

TABLE I: Best fit values of parameters entering in equation 4 fitted to the experimental deuteron energy spectra from this work compared to those obtained by Marion et al. [10].

TABLE II: Optical model potential parameters for the  ${}^3\text{He} + {}^7\text{Li}$  [49] and  $d + {}^8\text{Be}$  [50] elastic scattering reaction channels.

TABLE III: Ratios of the  $1p_{1/2}$  to  $1p_{3/2}$  shells partial DWBA differential cross sections and Cohen and Kurath shell model-calculated [54] spectroscopic factors for the three studied states of  ${}^8\text{Be}$ .

TABLE IV: Experimental  $C^2S$  global spectroscopic factor values for the three studied states of  ${}^8\text{Be}$  inferred in this work from our DWBA analysis of  ${}^7\text{Li}({}^3\text{He},d){}^8\text{Be}$  experimental data compared to Basak et al. experimental values [30] and to shell model calculated [13, 54] counterparts.

TABLE V: Experimental and shell model-predicted [54] partial spectroscopic factor values for the three studied states of  ${}^8\text{Be}$ .

TABLE VI:  $\gamma_p^2(a)$  proton-reduced widths versus the  $p + {}^7\text{Li}$  channel radius deduced in this work from our DWBA analysis of  ${}^7\text{Li}({}^3\text{He},d){}^8\text{Be}$  experimental data compared to shell model-predicted [14, 34] and R-matrix [57] counterparts.

### Figures captions:

FIG. 1: Part of the deuteron energy (position) spectrum recorded at  $\theta_{\text{lab}} = 5^\circ$  in our  ${}^7\text{Li}({}^3\text{He},d){}^8\text{Be}$  experiment.

FIG. 2 : Portion of the deuteron energy spectrum for  $\theta_{\text{lab}} = 35^\circ$  showing the  $2^+$  (16.626) and  $2^+$  (16.922) states of  ${}^8\text{Be}$  very well resolved due to the high energy resolution of the detection system used in this experiment. The solid curve represents the best fit to the experimental data points obtained from the Breit-Wigner two-level expression 4. The dotted curves represent the separate components associated with these two  $2^+$  states while the dashed curve describes their interference (last term in 4).

FIG. 3 : Experimental cross section angular distributions (scatter points) of the  $2^+$  (16.626) state of  ${}^8\text{Be}$ . The solid curve represents the best theoretical fit to experimental data from our FR-DWBA analysis (equation 8).

FIG. 4 : Same as FIG. 3 for the  $2^+$  (16.922) state of  ${}^8\text{Be}$ .

FIG. 5 : Same as FIG. 3 for the  $1^+$  (17.640) state of  ${}^8\text{Be}$ .

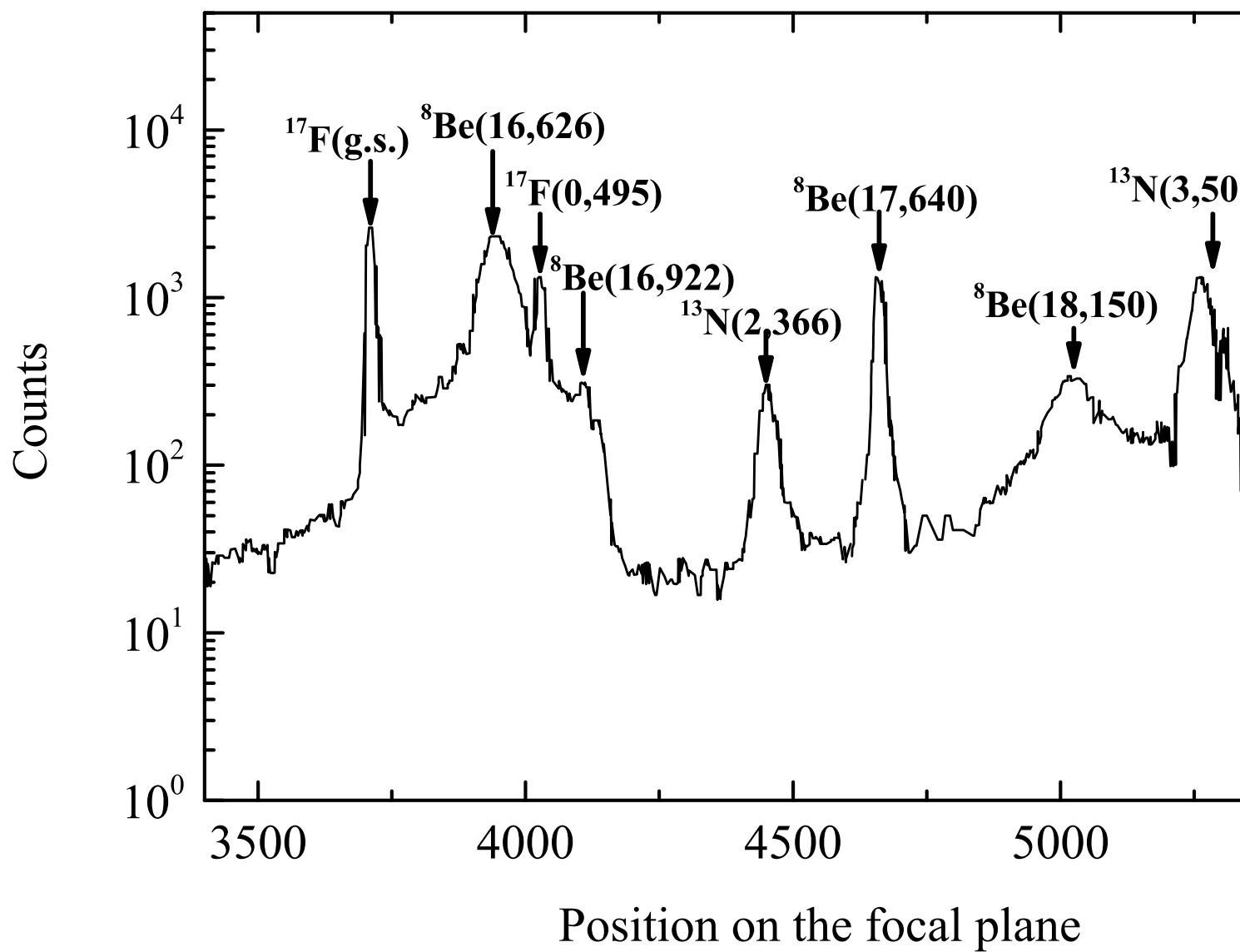


FIG. 1; A. Belhout et al.

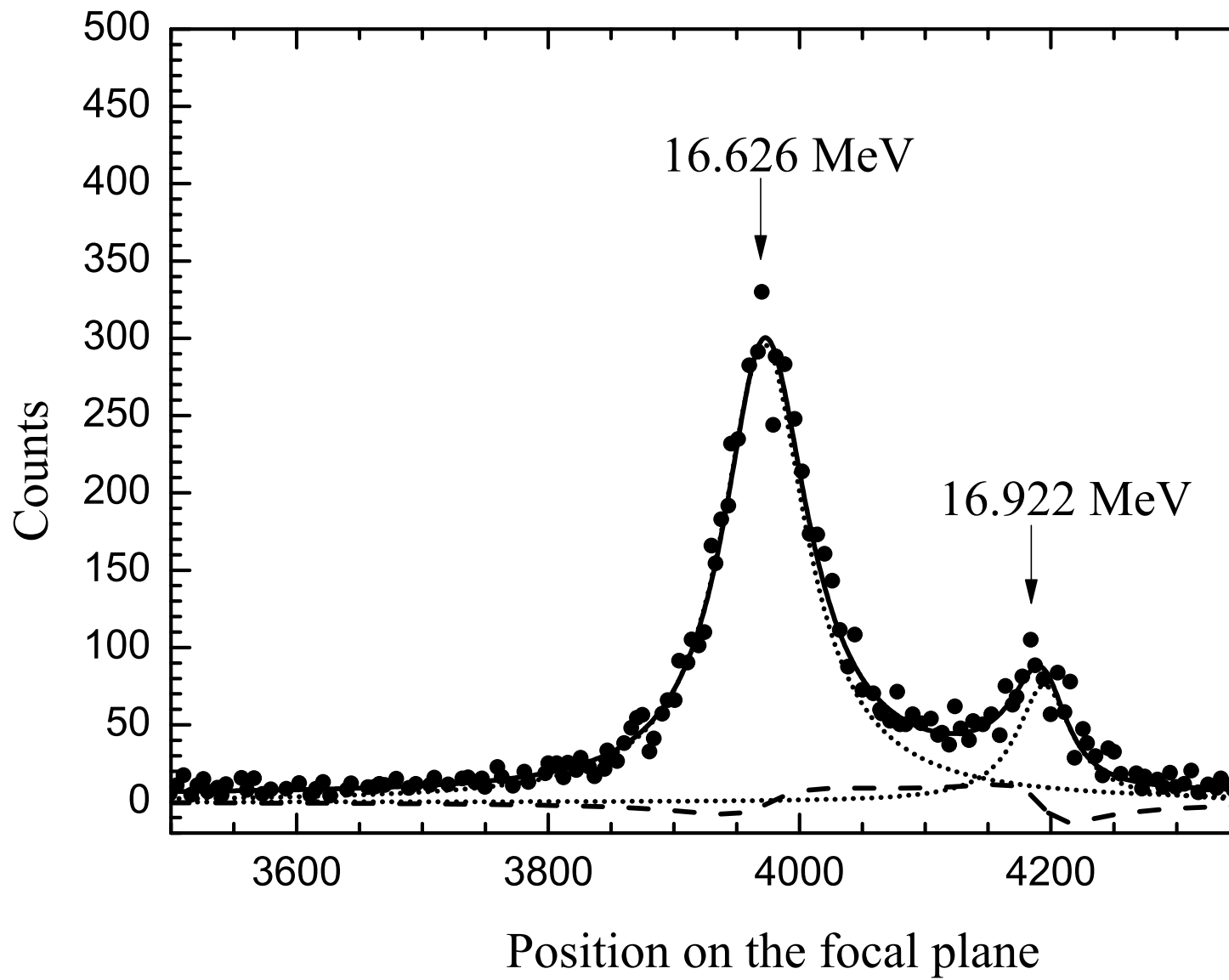


FIG. 2; A. Belhout et al.



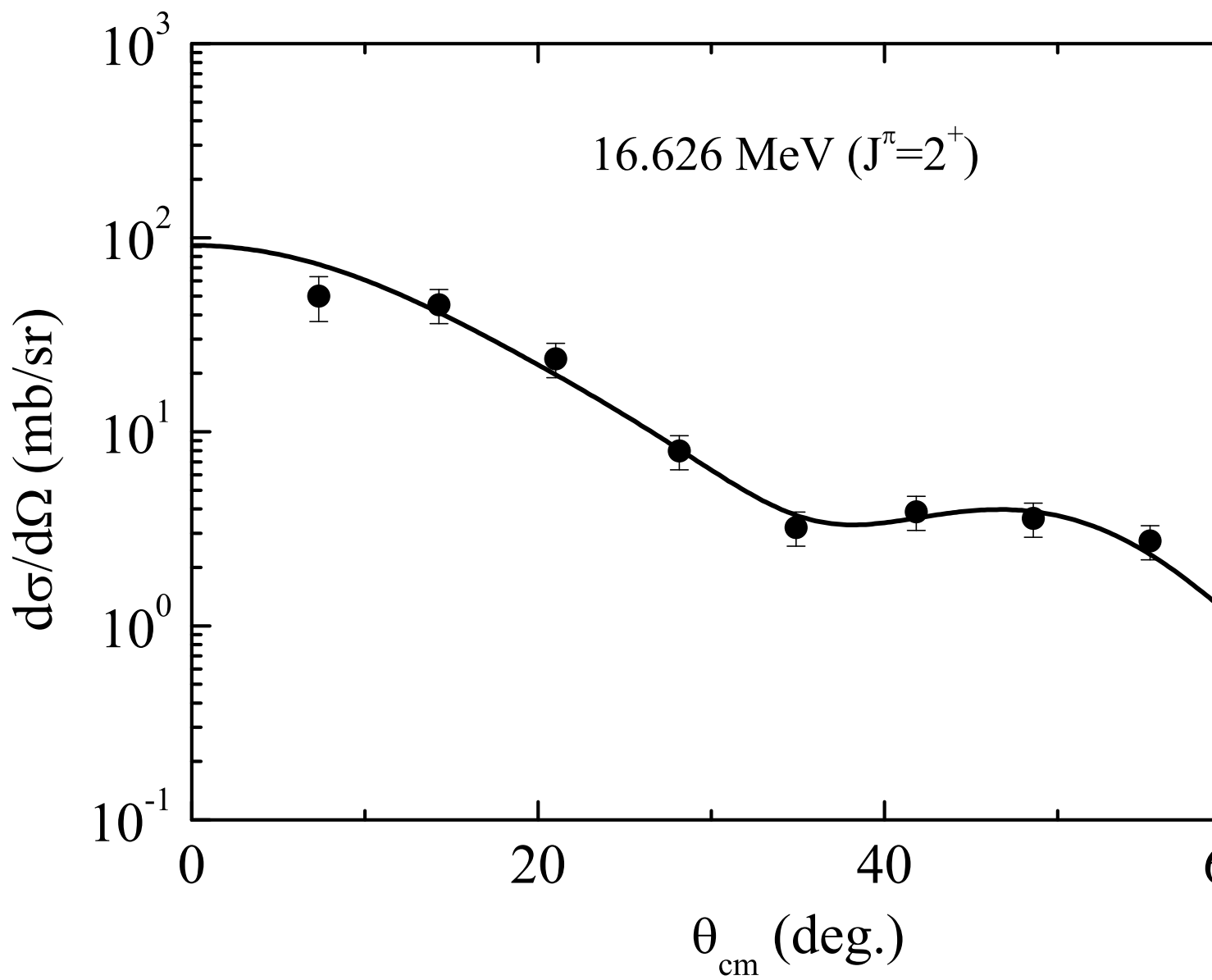


FIG. 3; A. Belhout et al.

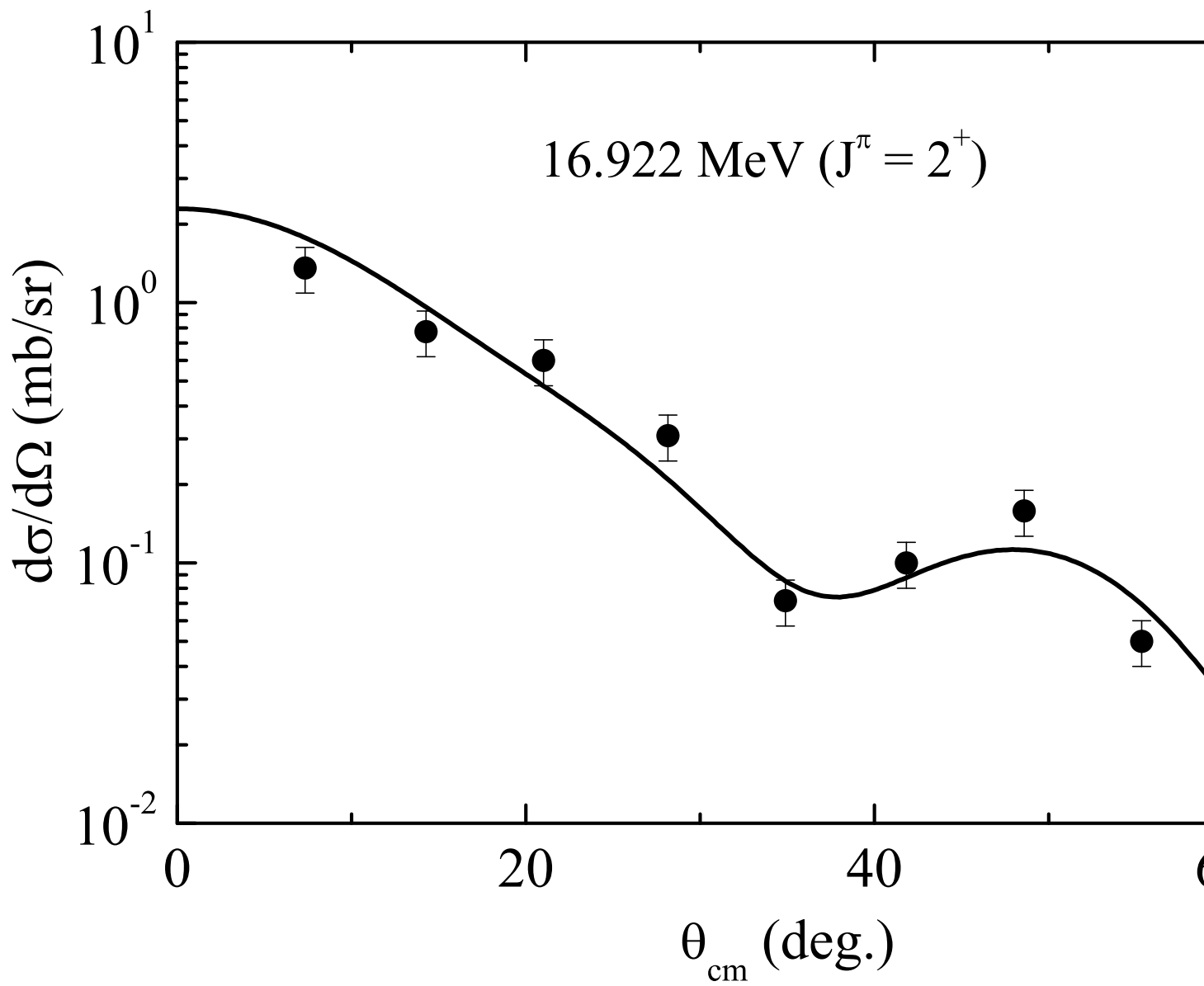


FIG. 4; A. Belhout et al.

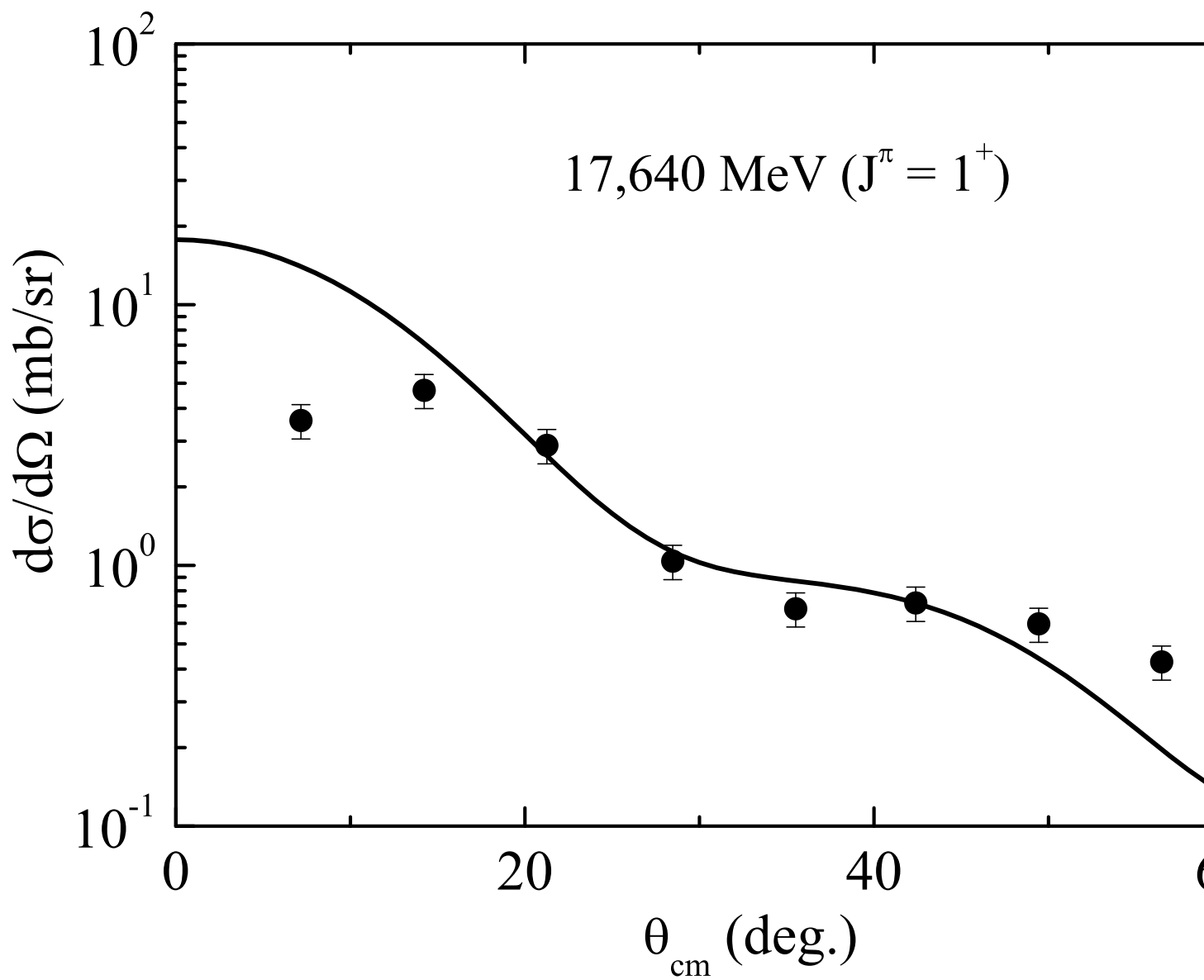


FIG. 5; A. Belhout et al.